Hungarian Space Office

SZENT ISTVÁN UNIVERSITY

esa

→ 7th ADVANCED TRAINING COURSE ON LAND REMOTE SENSING

4–9 September 2017 | Szent István University | Gödöllő, Hungary

URBAN MAPPING AND CHANGE DETECTION

Sebastian van der Linden
with contributions from Akpona Okujeni

Humboldt-Unveristät zu Berlin, Germany

Introduction

Introduction – The urban millennium

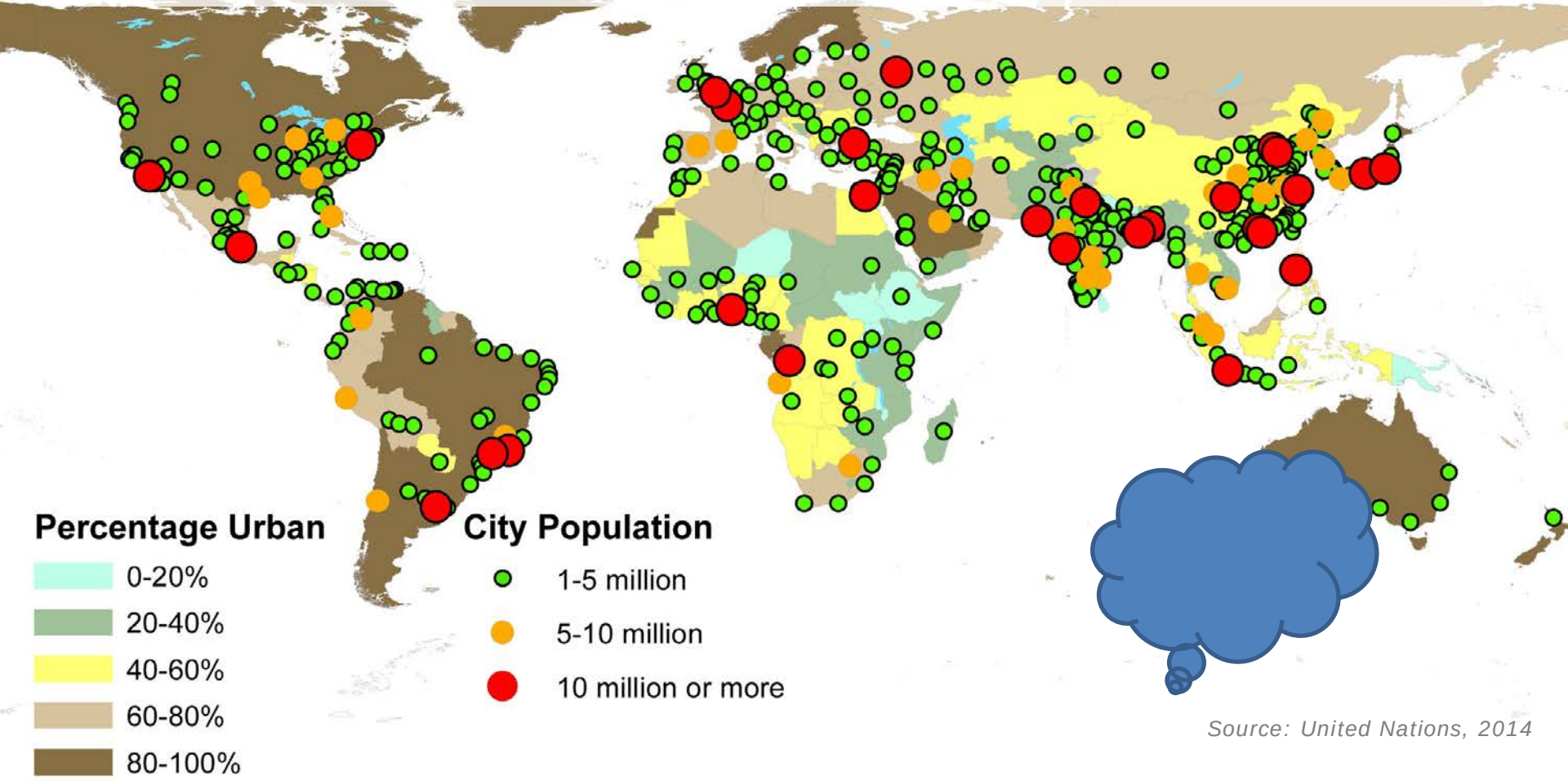

Source: United Nations, 2014

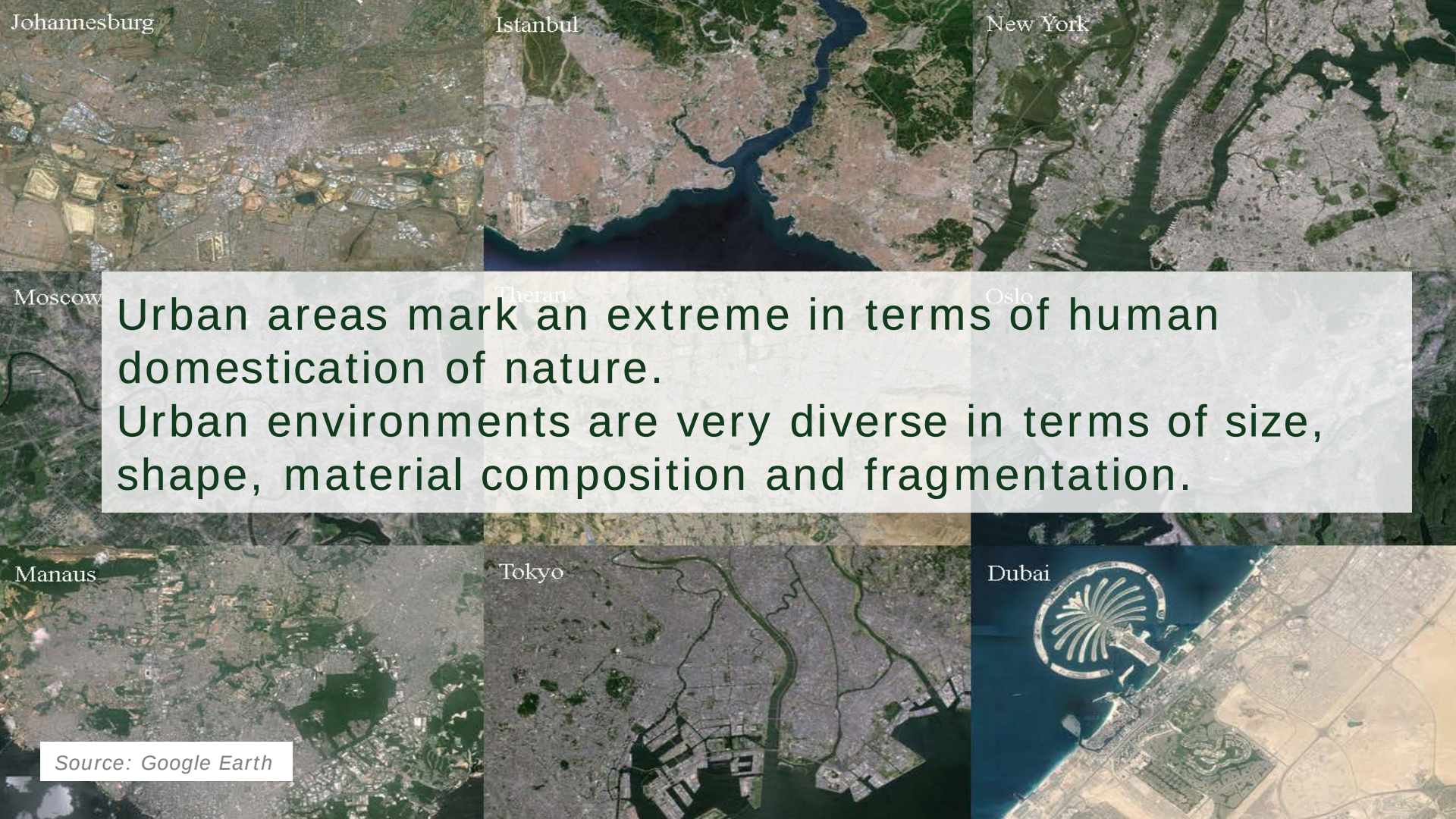

Urban areas mark an extreme in terms of human domestication of nature.
Urban environments are very diverse in terms of size, shape, material composition and fragmentation.

Source: Google Earth

Berlin-Brandenburg area in Global Urban Footprint TerraSAR-X product of DLR

Urban environments are not fully composed of built-up structures or impervious areas.
Different sensors contribute differently to mapping urban extent and urban composition.

Source: www.dlr.de

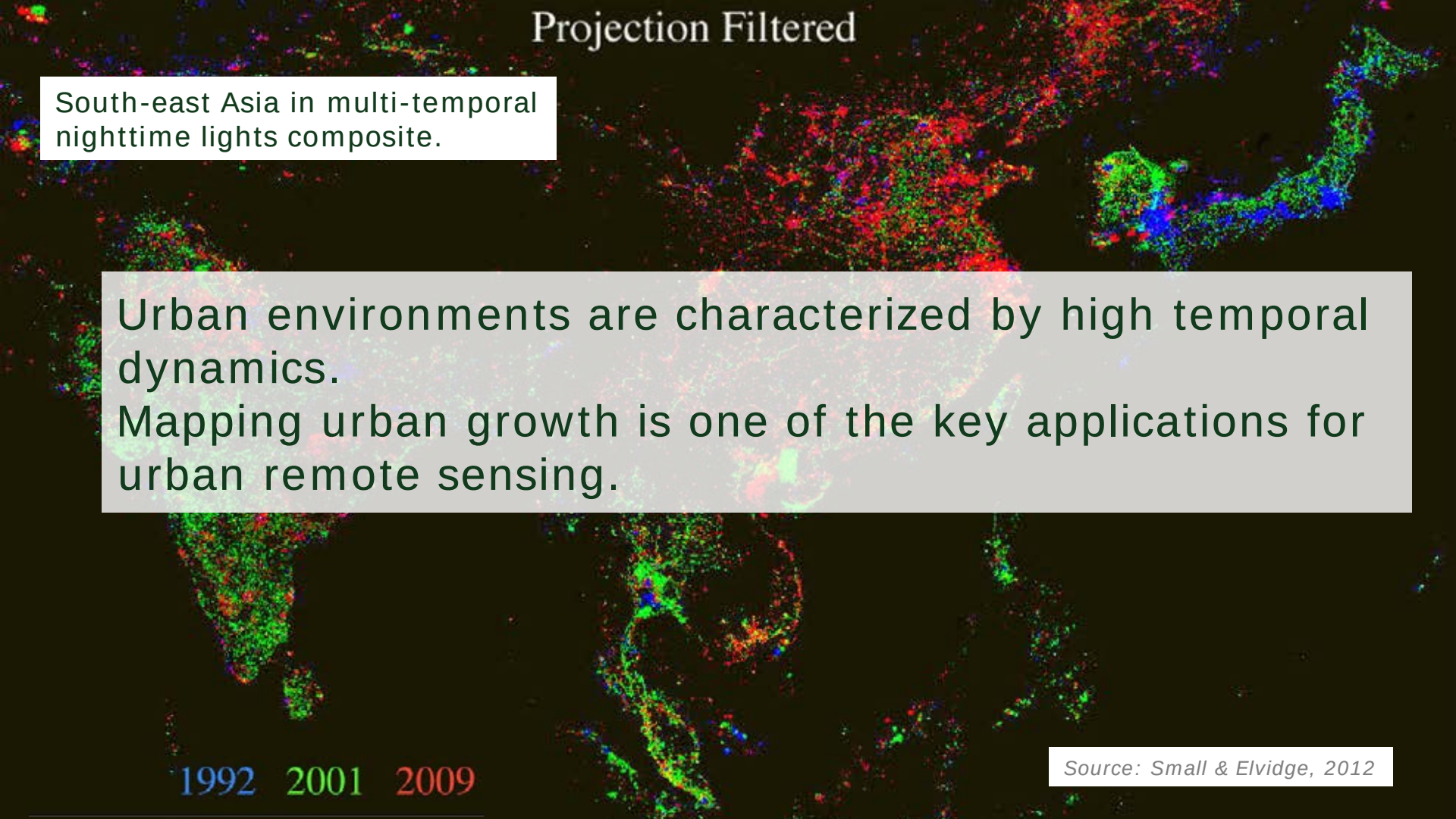

South-east Asia in multi-temporal nighttime lights composite.

Urban environments are characterized by high temporal dynamics.
Mapping urban growth is one of the key applications for urban remote sensing.

Source: Small & Elvidge, 2012

Urban material composition influences the micro climate and other environmental variables.

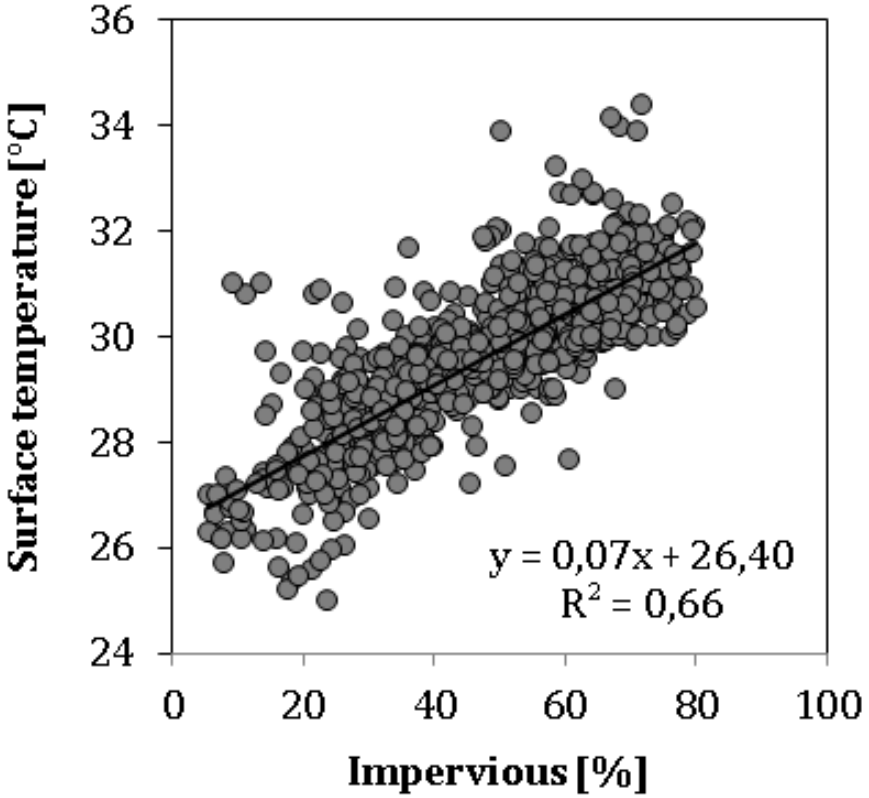

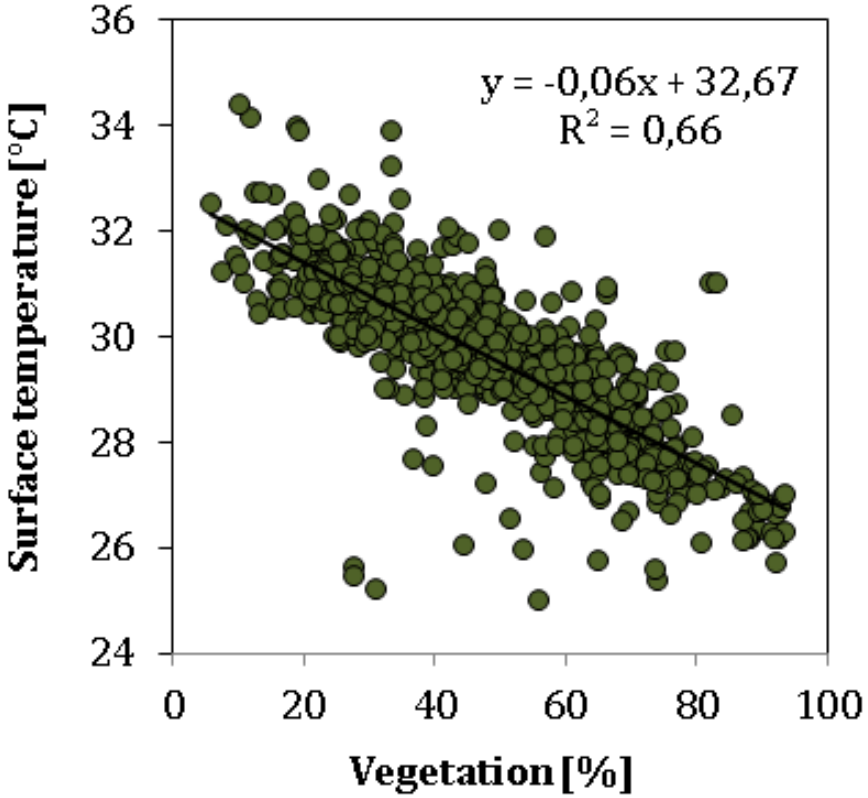

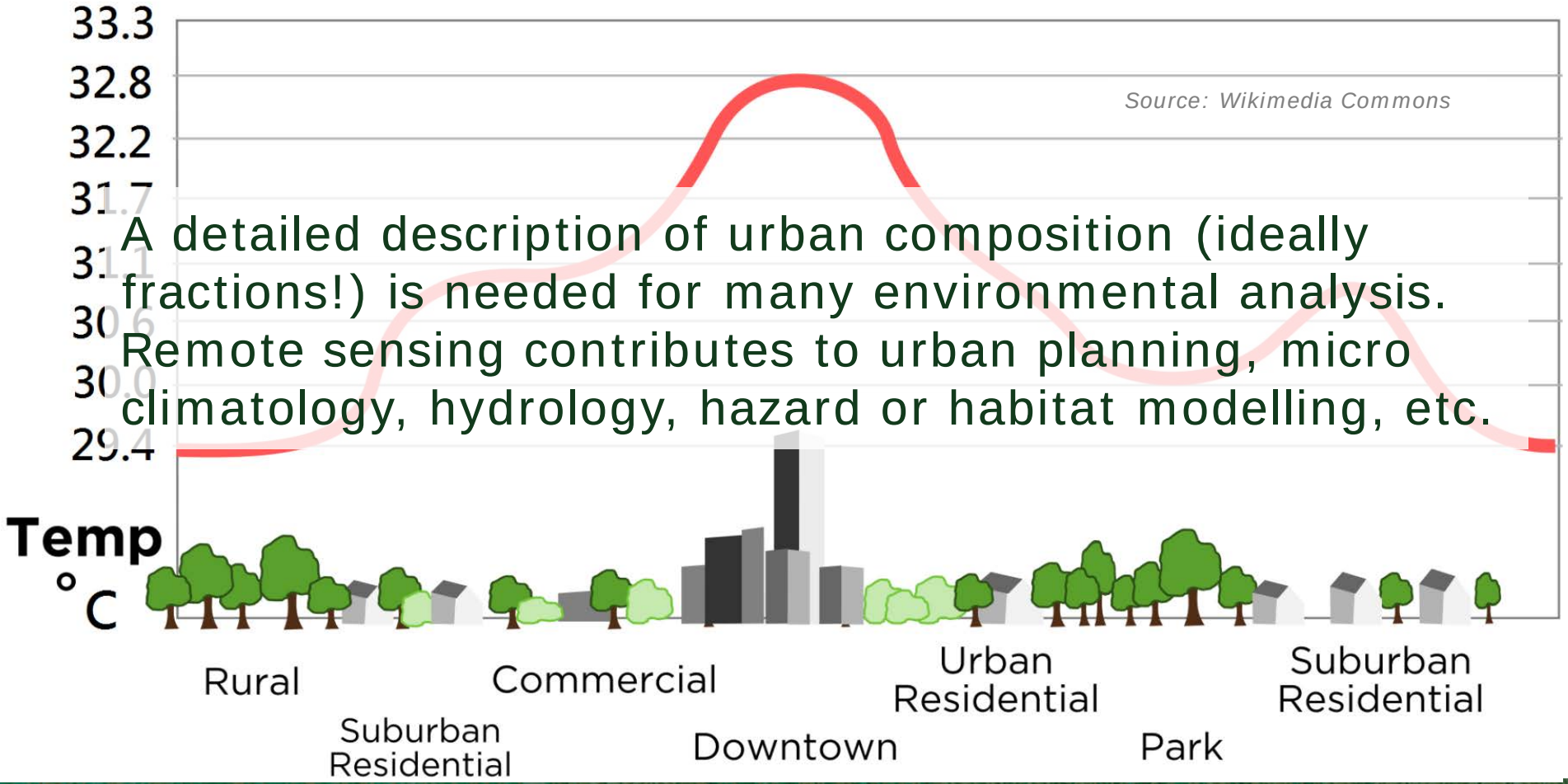

A detailed description of urban composition (ideally fractions!) is needed for many environmental analysis. Remote sensing contributes to urban planning, micro climatology, hydrology, hazard or habitat modelling, etc.

Introduction (summary)

With more than have of the world's population living in cities and rapid urbanization rates, remote sensing plays a pivotal role in monitoring urban environments.

Especially in less developed countries and for fast growing urban agglomerations remote sensing is often the only reliable source of spatial information.

Most urban environmental models use remotely sensed maps as input.

Remote sensing analyses usually focus on

- mapping urban extent and growth
- mapping urban composition

Characteristics and challenges of urban land cover and urban remote sensing

Urban land cover

Urban land cover is characterized by great diversity of materials.

Source: Google Earth

Urban land cover

Urban land cover is characterized by high intra-class variation and often spectral ambiguity between classes.

Landsat ETM+ (30 m; 6 spectral bands)

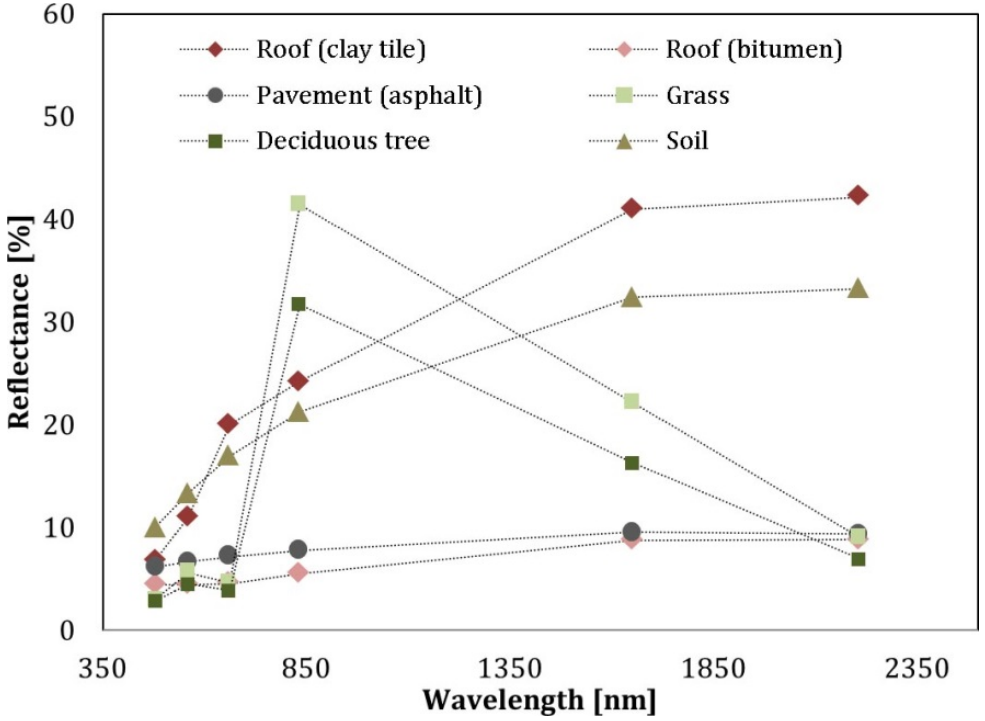

Urban land cover

Urban land cover classes can be hierarchically organized down to the material level.

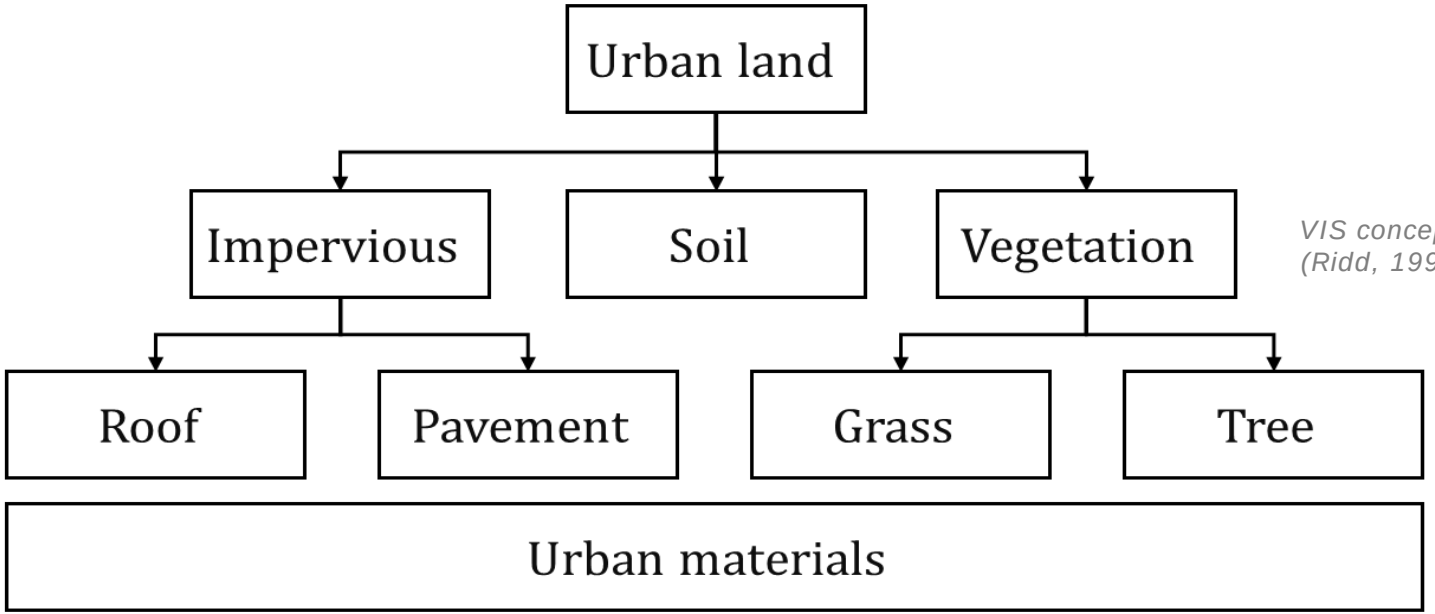

VIS concept (Ridd, 1995)

Urban land cover

High spectral diversity of construction materials and natural surface types.

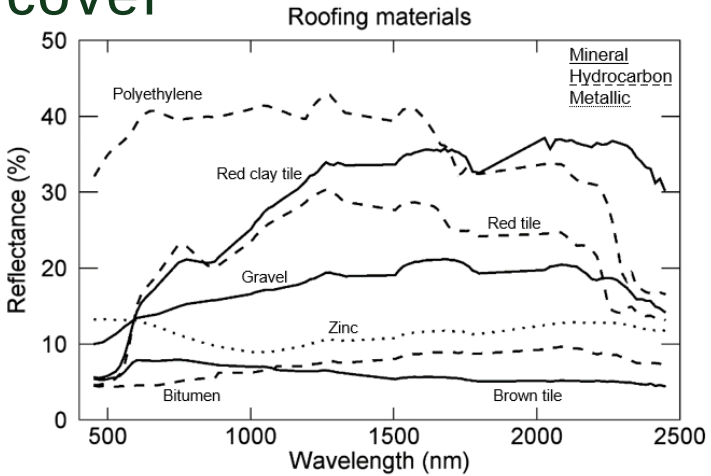

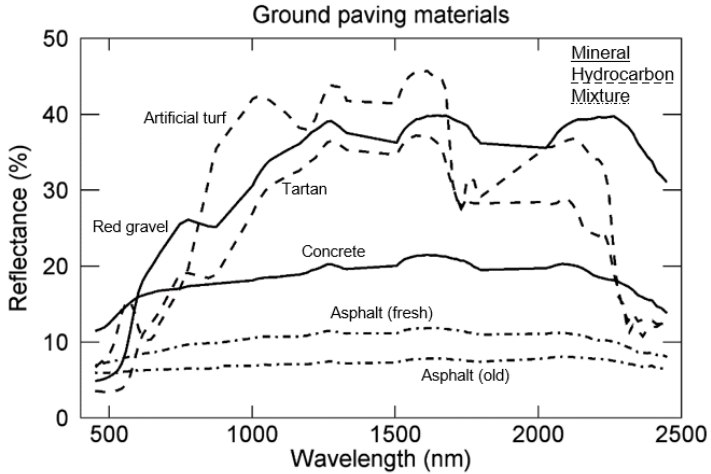

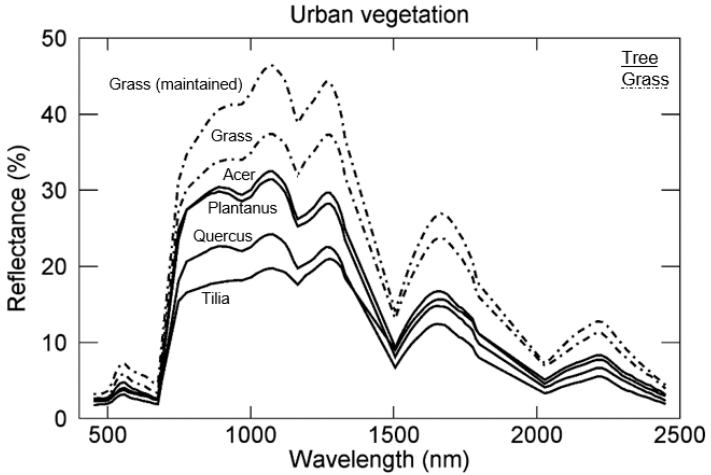

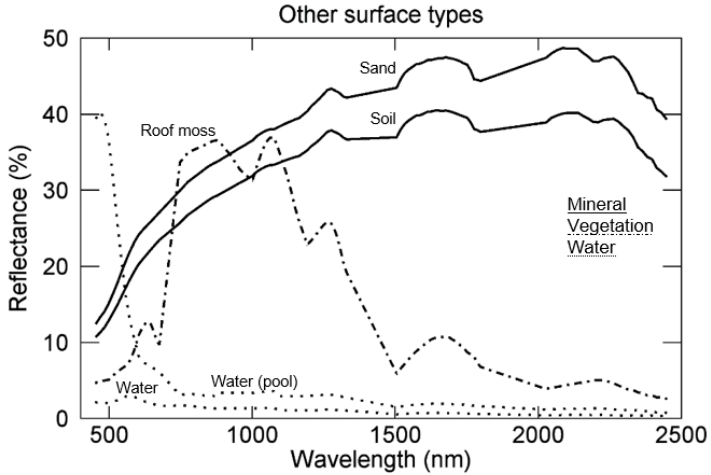

Source: Small et al., in press

→ 7th ADVANCED TRAININ
4–9 September 2017 | Szent István

Urban land cover

30x30 km footprint of Berlin, Germany, as seen by

UL: Landsat 8 (swIR, nIR, red)

UR: Landsat 8 thermal

LL: Sentinel-1A

LR: vis. nightlights (ISS photo).

Each observation provides complementary information, but is also subject to non-uniqueness.

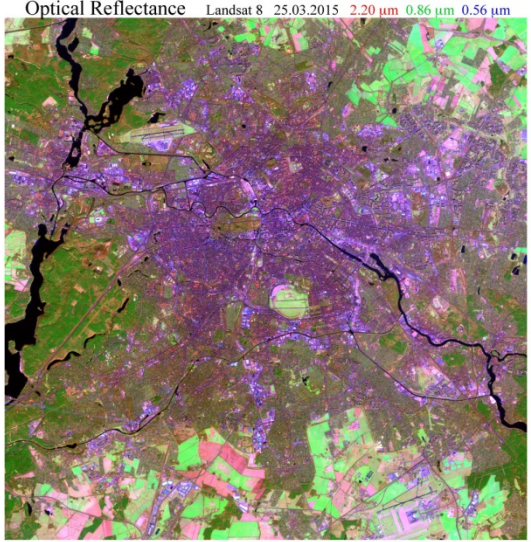

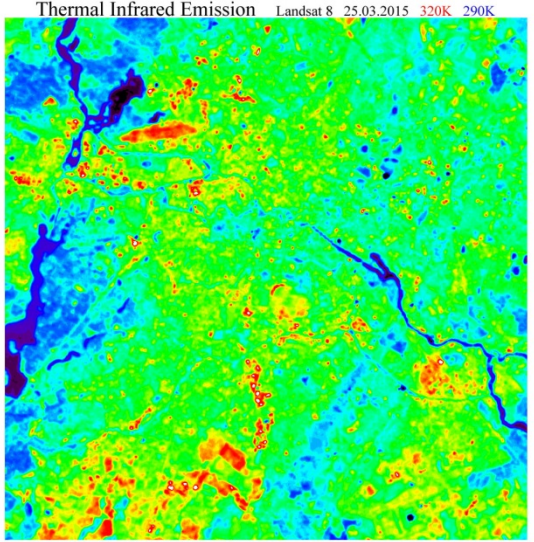

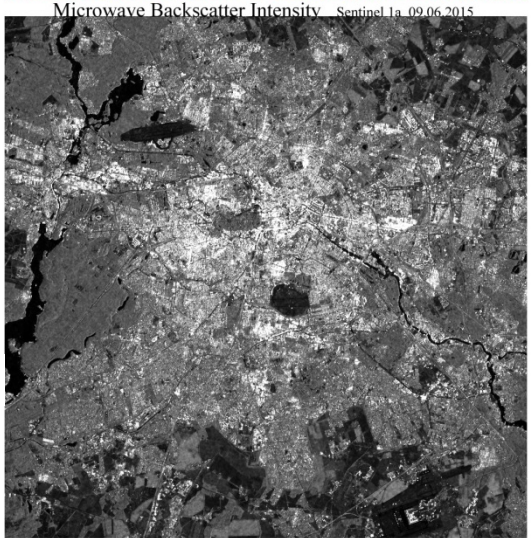

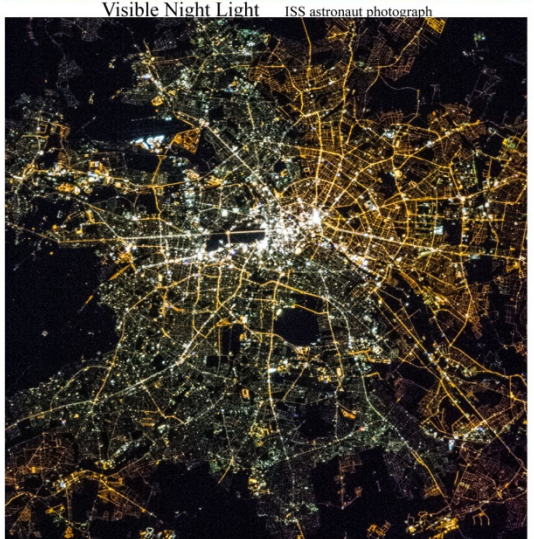

Source: Small et al., in press

Urban land cover

Polarimetric representation of Berlin area and three subsets using TerraSAR-X StripMap data in the Pauli color coding scheme (R: HH-VV, G: HV, B: HH+VV).

Mirror-like reflectors appear dark (streets, sport fields, water). Vegetation is greenish with HV dominating. Strong backscatter structure appear bright with the actual color also depending on object size, geometric arrangement and orientation.

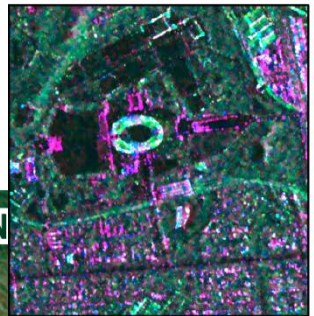

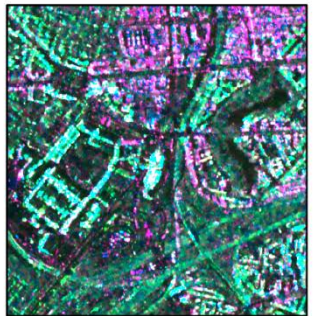

Source: Small et al., in press

Urban land cover

Berlin area thermal emissions in July and September during day (middle) and night (bottom). Landsat 7 for comparison (top).

Water bodies show low values at day and highest at night. Urban forests are always in mid-ranges. Street canyons and large buildings store energy longer and emit even at nighttime.

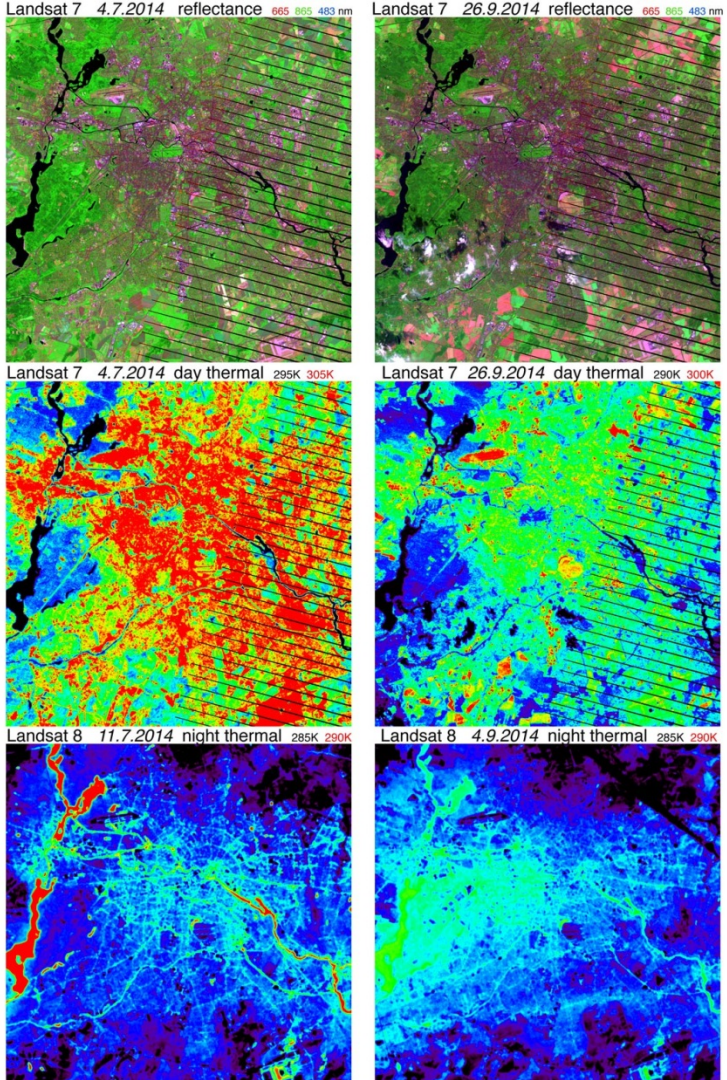

Source: Small et al., in press

The factor scale in urban remote sensing

Step from approx. 5 m to 30 m leads to massive spatial aggregation.

Aerial photograph 0.2 m 21.07.2015

HyMap 3.6 m 20.08.2009

Sentinel-2 10 m 23.08.2015

Source: Small et al., in press

The factor scale in urban remote sensing

Step from approx. 5 m to 30 m leads to massive spectral aggregation.

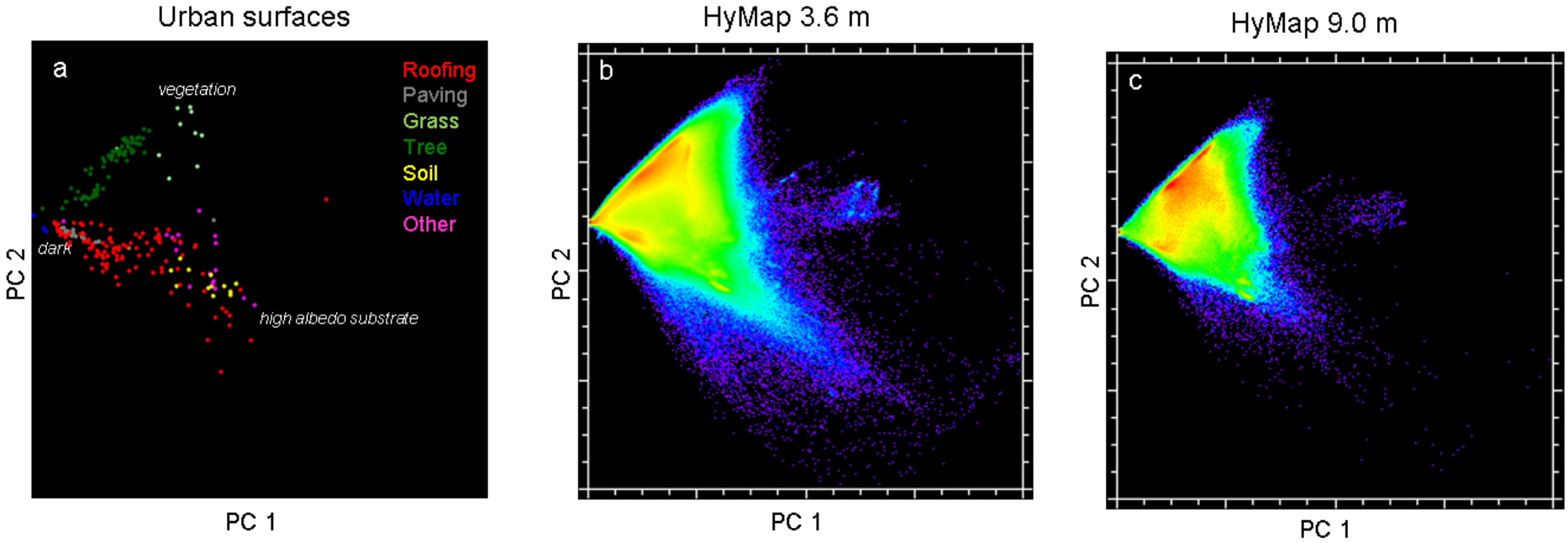

Source: Small et al., in press

The factor scale in urban remote sensing

High number of mixed pixels.

Complex 3-D geometry and illumination.

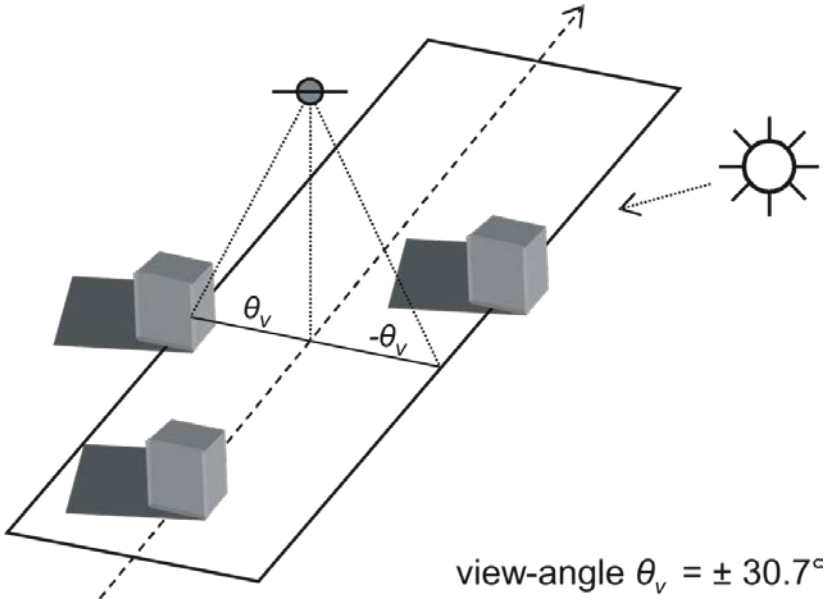

view-angle $\theta_v = \pm 30.7^c$

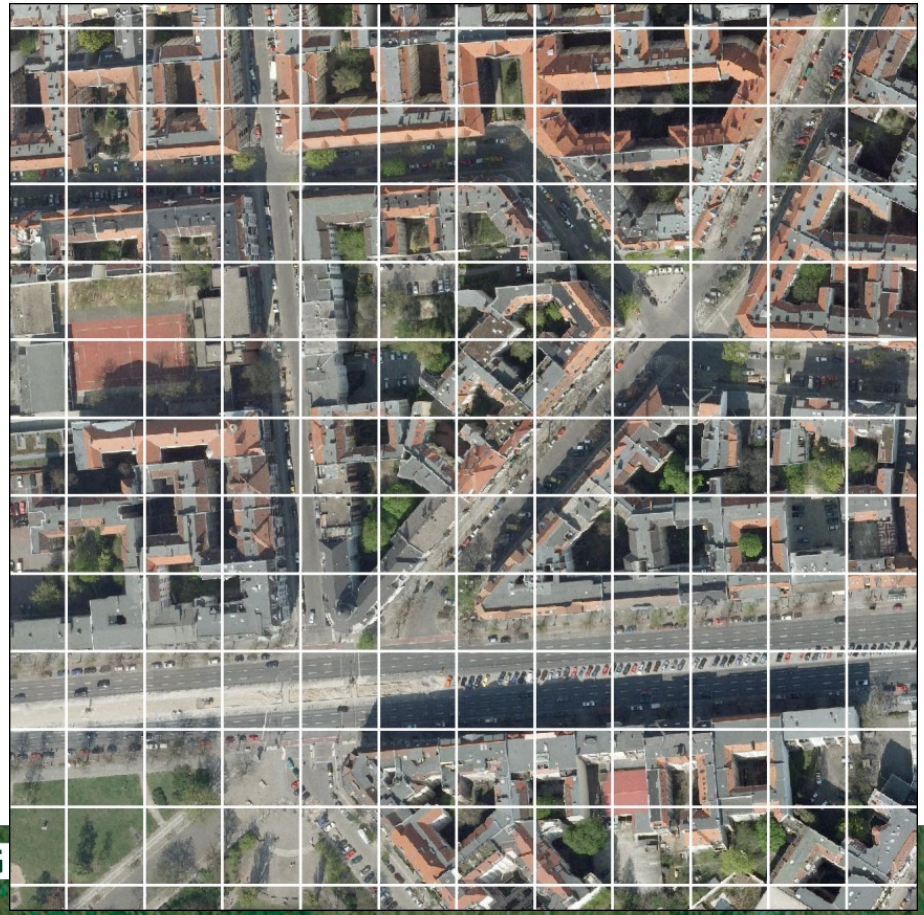

Mapping urban growth

Mapping urban growth from optical and SAR data

Urban growth can be mapped reliably by means of remote sensing.

Taubenböck et al. (2012) use data from TerraSAR-X and Landsat to quantify urban growth for global mega cities since 1975 in four time steps.

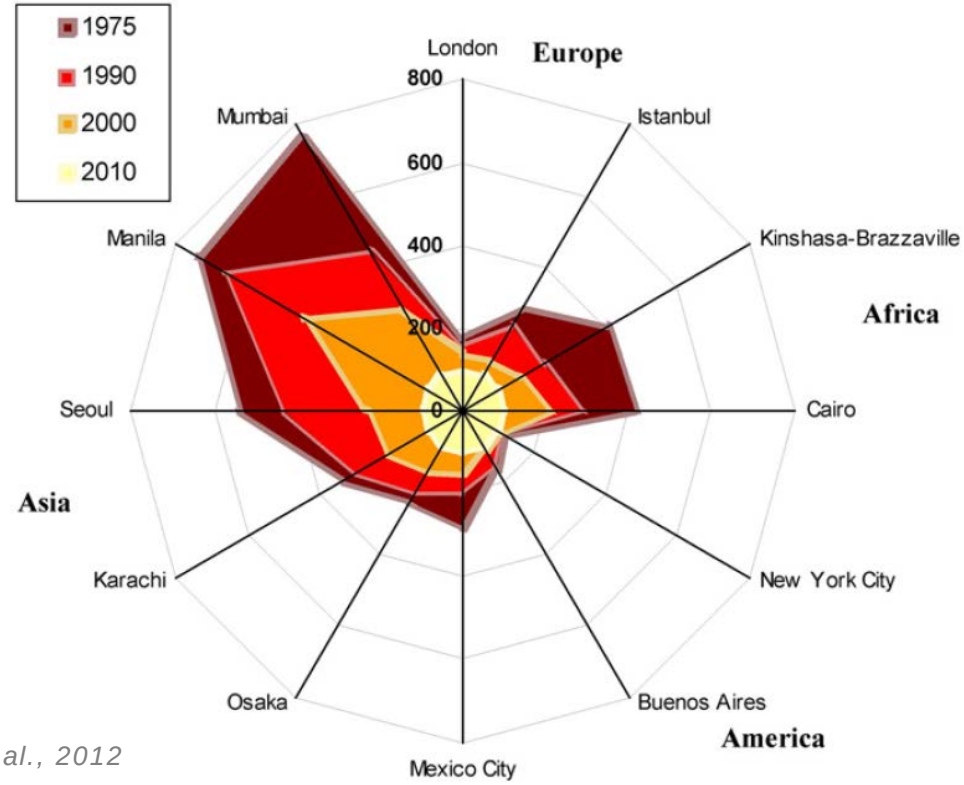

Source: Taubenböck et al., 2012

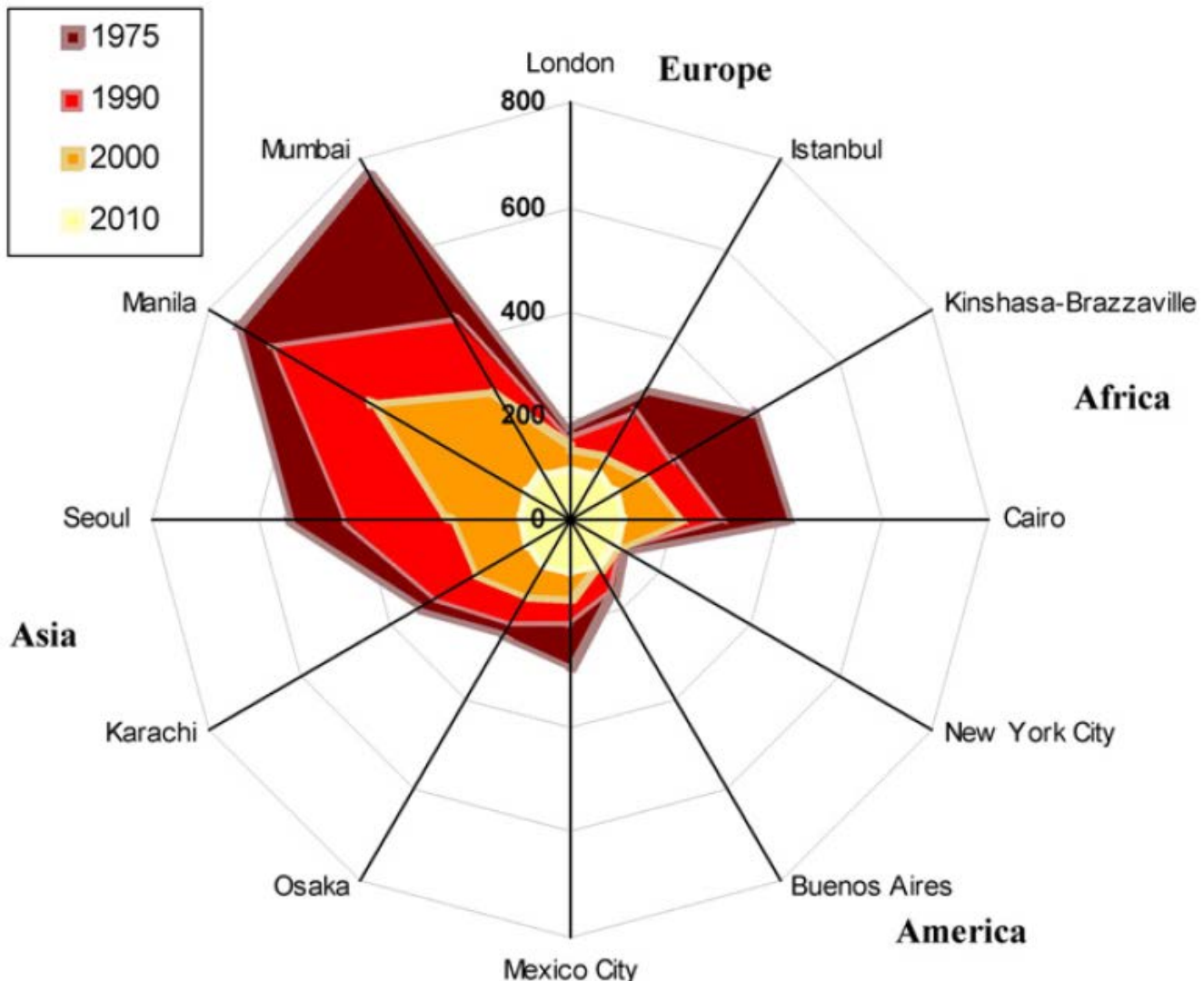

Mega cities are mapped in
1975 – Landsat MSS
1990 – Landsat TM
2000 – Landsat ETM+
2010 – TerraSAR-X

Source: Taubenböck et al., 2012

Map of Karachi, Pakistan

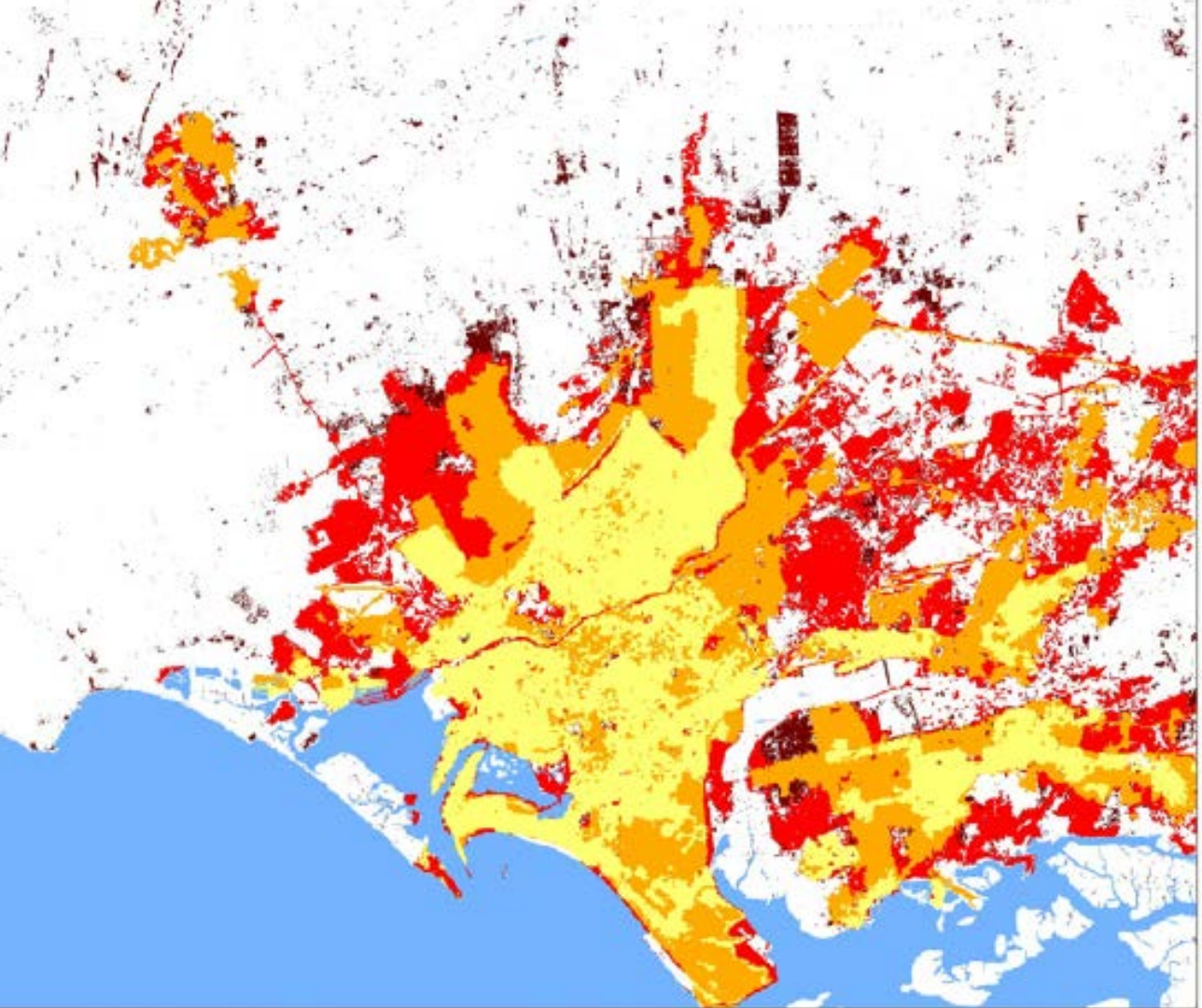

Source: Taubenböck et al., 2012

Mapping urban growth from optical and SAR data

Landsat and TerraSAR data are classified with different approaches.

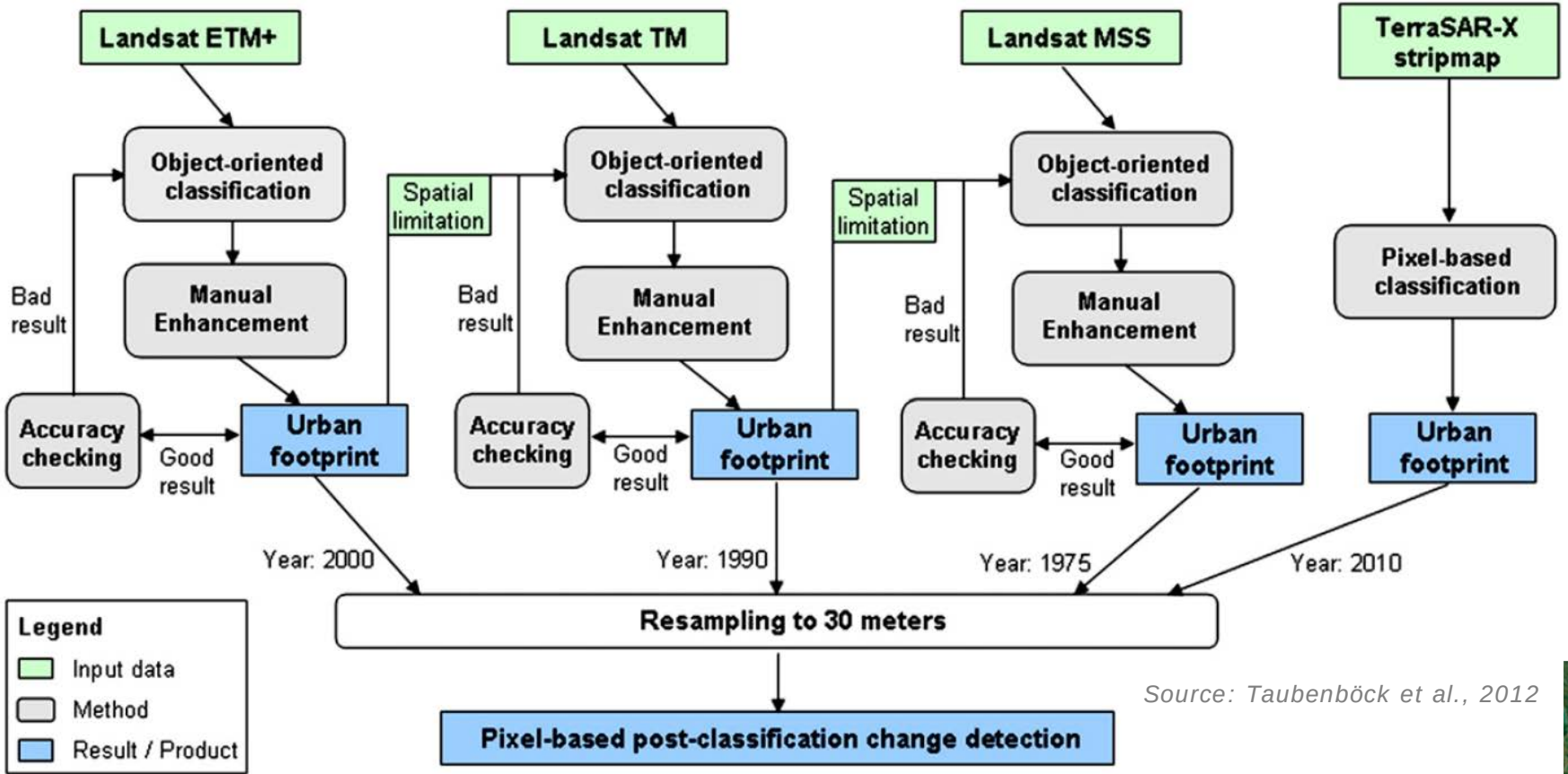

Source: Taubenböck et al., 2012

Mapping urban growth from spectral and SAR data

Griffiths et al. (2010) monitor the growth of Dhaka, Bangladesh, for 1990, 2000 and 2006 based on Landsat TM/ETM+ and ERS-1/ASAR data.

By fusing the multispectral optical and the SAR data they can map urban extent reliably in this heavily monsoon and flooding influenced area of rapid urbanization.

Both sensor types contribute to the high overall accuracy.

2006 – Results of feature selection – 2 classes

#1	ETM+(27.01.06) b6	72.3
#2	SAR (02.12.07) HH	90.1
#3	ETM+(27.01.06) b4	92.1
#4	SAR (31.10.07) HH	93.0
#5	ETM+(13.12.2006) b3	93.4
#6	ETM+(27.01.06) b5	93.6
#7	ETM+(13.12.2006) b5	93.8

Source: Griffiths et al., 2010

Mapping urban growth from spectral and SAR data

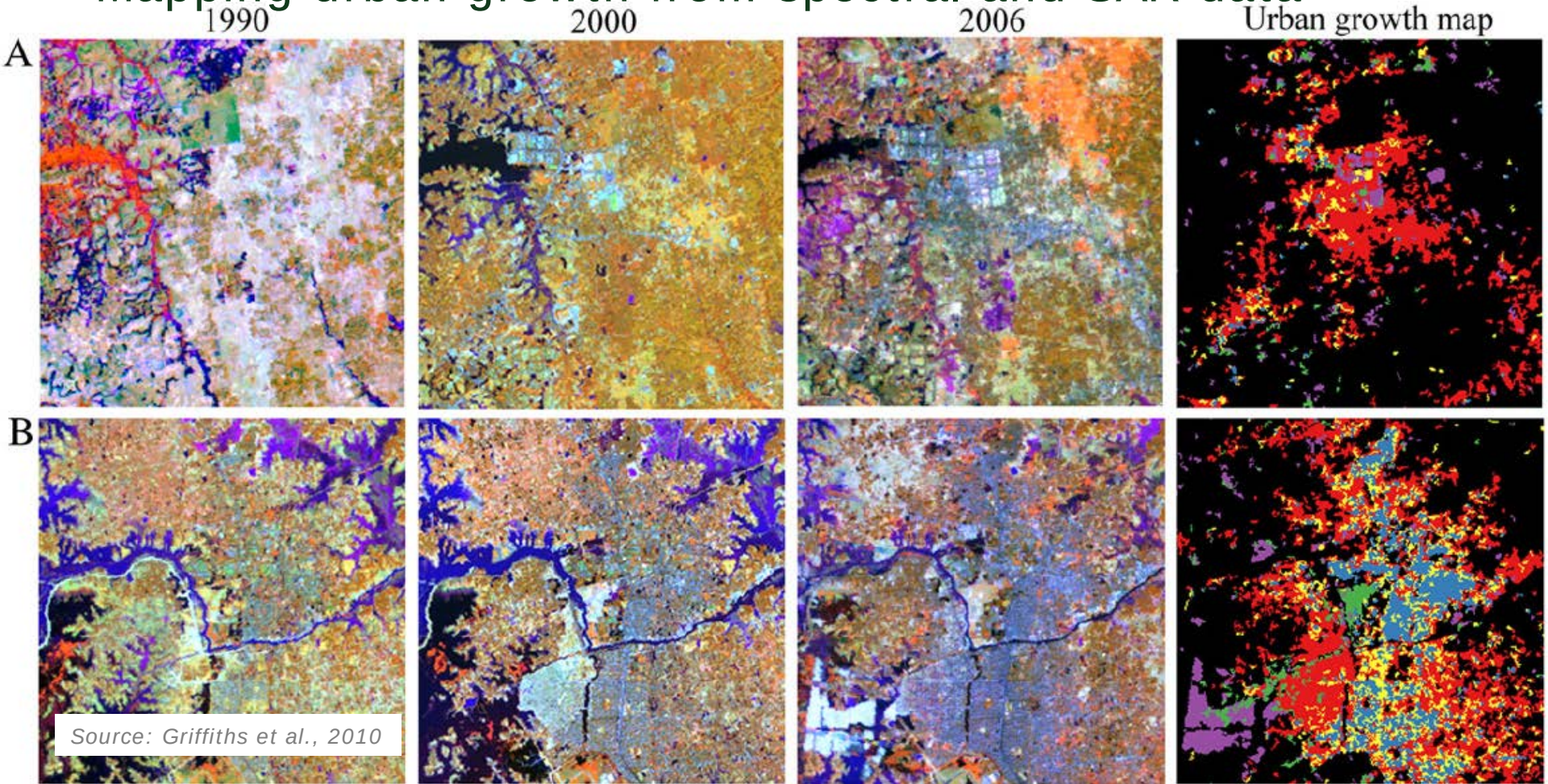

Mapping urban composition

Mapping urban composition from spectral data

Ridd (1995) assumes, every urban pixel is composed of impervious surface, vegetation or soil.
Ridd's V-I-S concept is based on a thematical framework. It is not based on the spectral characteristics of urban areas.

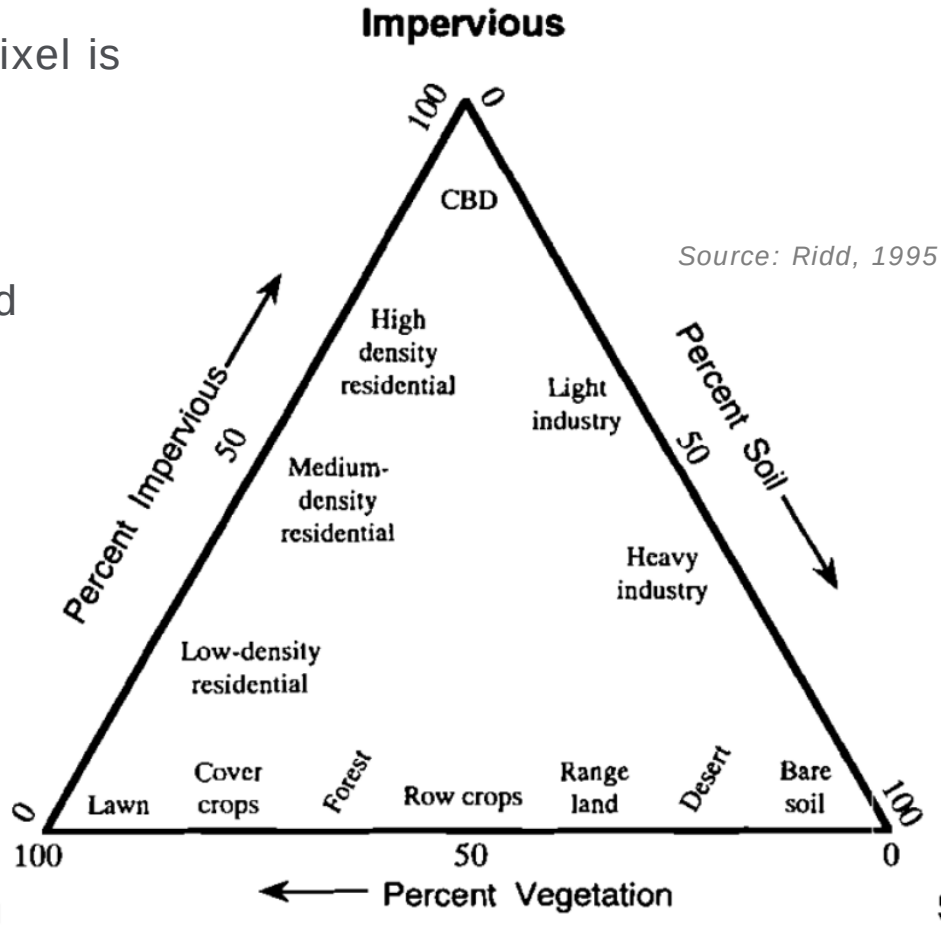

Source: Ridd, 1995

Mapping urban composition from spectral data

Small (2005) analyses more than 24 urban areas and concludes that the spectral properties working with Landsat ETM+ always relate to the degree of brightness and the portion of vegetation. This results in a mixing triangle in the first Two PC components.

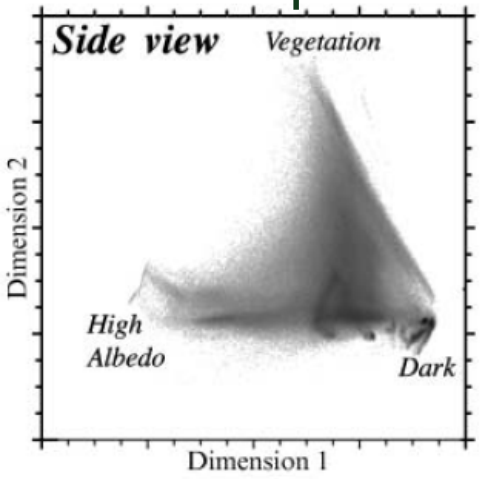

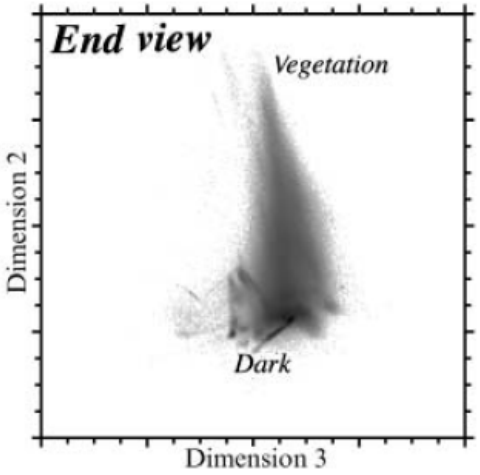

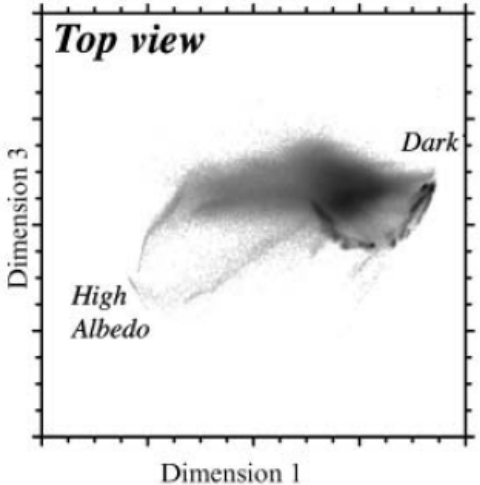

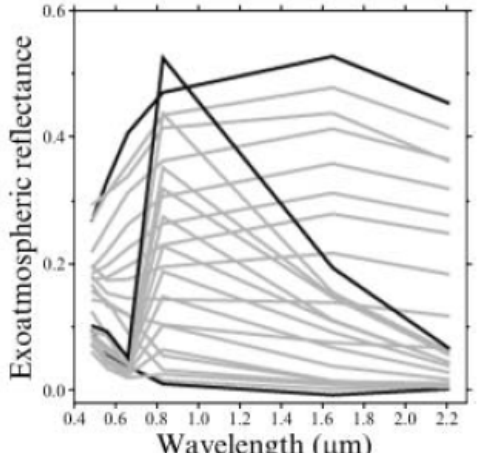

Source: Small, 2005

Mapping urban composition from spectral data

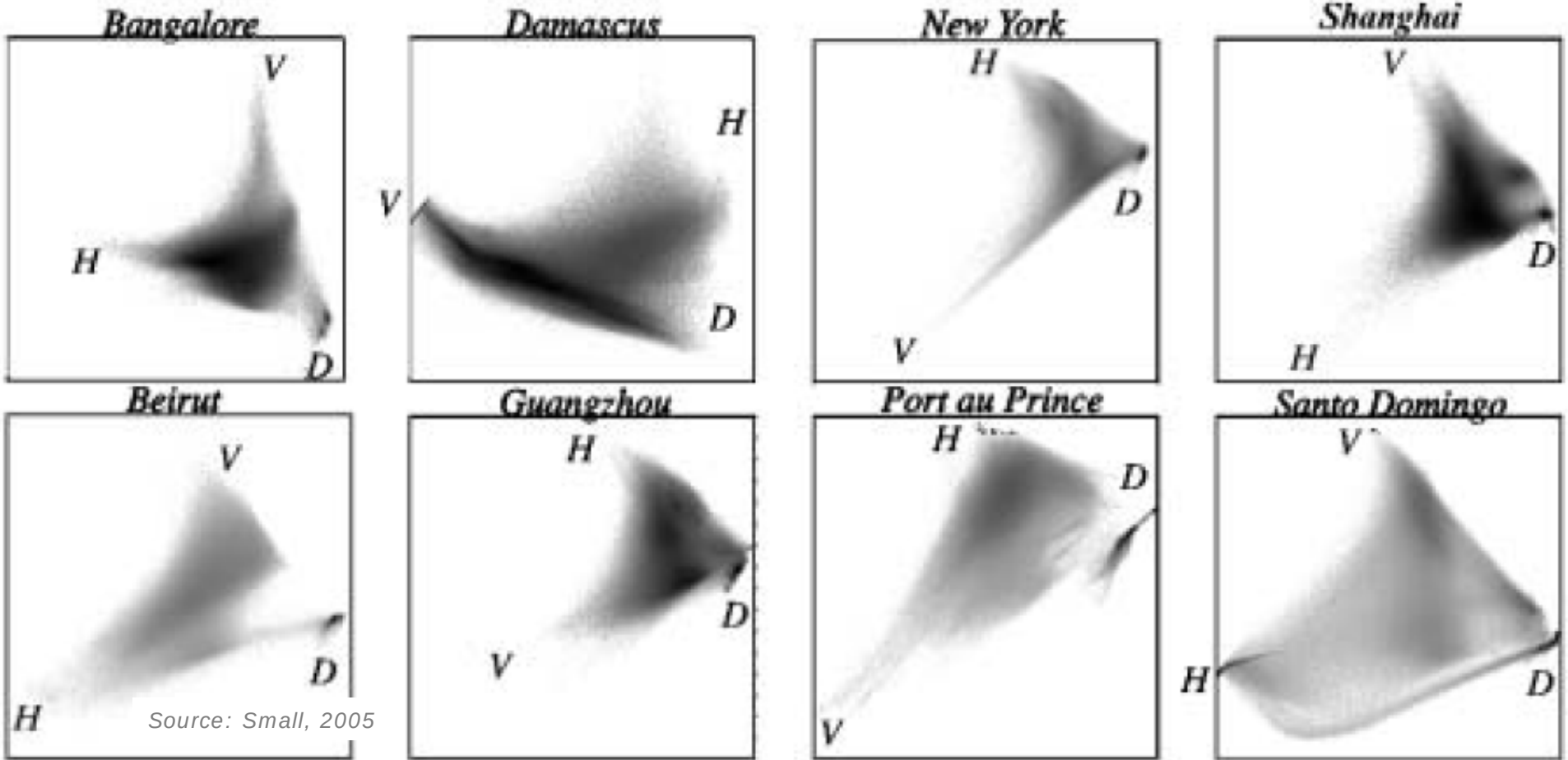

Source: Small, 2005

Mapping urban composition from spectral data

Using higher spatial and spectral characteristics and machine learning, van der Linden et al. (2007) showed that more urban cover types can be mapped.

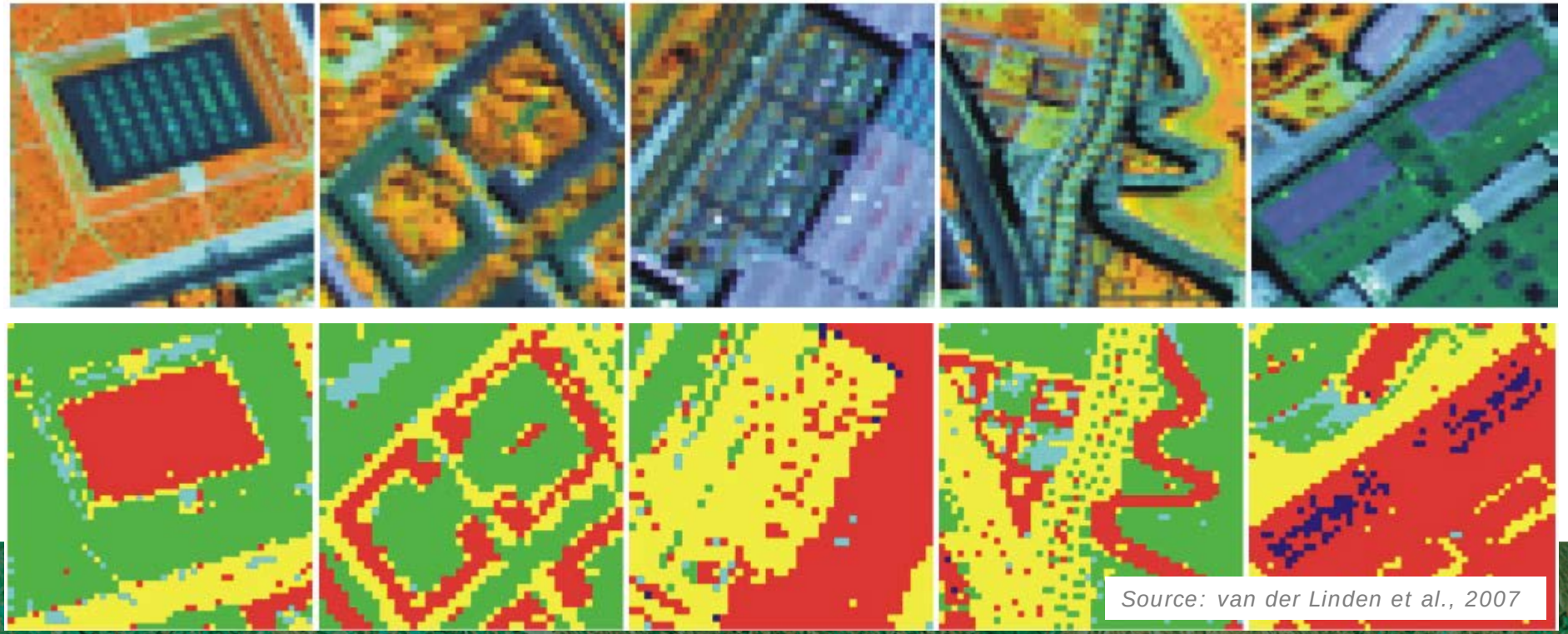

Source: van der Linden et al., 2007

Mapping urban composition using spectral and lidar data

Land cover maps from APEX (2 m; 252 bands) and LiDAR data.

SVC classification with post-processing.

Height/shadow information to account for spectral ambiguity.

High share of pure pixels and high Accuracies.

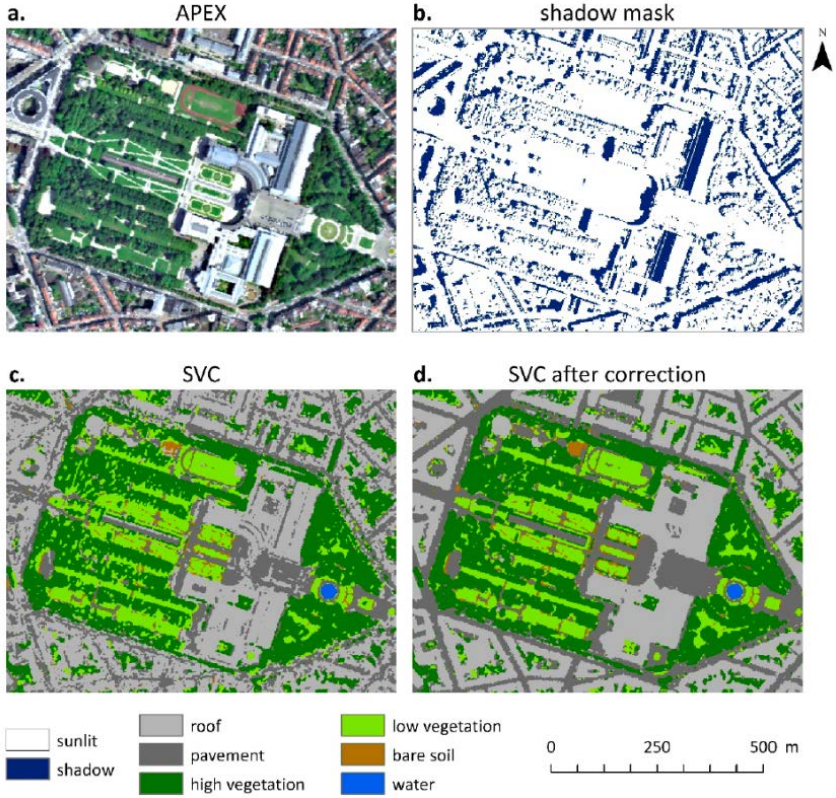

Source: Priem & Canters, 2016

Land Cover	SVC	Cor. (Height)	Cor. (Slope)	Cor. (Roughness)	Cor. (All)
1. red ceramic tile	0.82	0.82	**0.88**	0.82	**0.88**
2. dark ceramic tile	0.81	0.95	**0.95**	0.81	**0.99**
3. dark shingle	0.51	0.51	**0.94**	0.50	**0.94**
4. bitumen	0.77	0.79	**0.90**	0.76	**0.93**
5. fiber cement	0.85	0.84	0.79	0.85	*0.75*
6. bright roof material	0.55	**0.64**	0.55	0.55	**0.63**
7. reflective hydrocarbon	0.75	**0.90**	0.81	0.73	**0.95**
8. gray metal	0.82	0.83	0.78	0.82	0.76
9. green metal	0.95	0.97	0.97	0.95	0.97
10. paved roof	0.87	0.89	0.87	0.87	0.88
11. glass	0.91	0.89	0.91	0.91	0.89
12. gravel roofing	0.71	**0.81**	0.69	0.70	**0.83**
13. extensive green roof	0.84	**1.00**	0.83	0.84	**1.00**
14. solar panel	1.00	1.00	*0.96*	1.00	*0.95*
15. asphalt	0.90	**0.98**	0.92	0.95	0.92
16. concrete	0.52	**0.71**	**0.62**	0.51	0.71
17. red concrete pavers	0.83	**1.00**	0.78	0.79	1.00
18. railroad track	0.83	*0.70*	0.80	0.98	**0.98**
19. cobblestone	0.59	0.75	0.53	0.62	**0.69**
20. bright gravel	0.90	*0.72*	0.90	0.90	*0.72*
21. red gravel	0.96	0.96	**1.00**	0.96	*0.89*
22. tartan	1.00	1.00	1.00	1.00	1.00
23. artificial turf	0.98	0.98	*0.93*	0.98	0.97
24. green surface	1.00	1.00	1.00	1.00	1.00
25. high vegetation	1.00	0.85	1.00	1.00	1.00
26. low vegetation	0.80	**0.94**	0.80	0.80	**0.94**
27. bare soil	0.93	*0.85*	0.92	0.93	*0.85*

Source: Priem & Canters, 2016

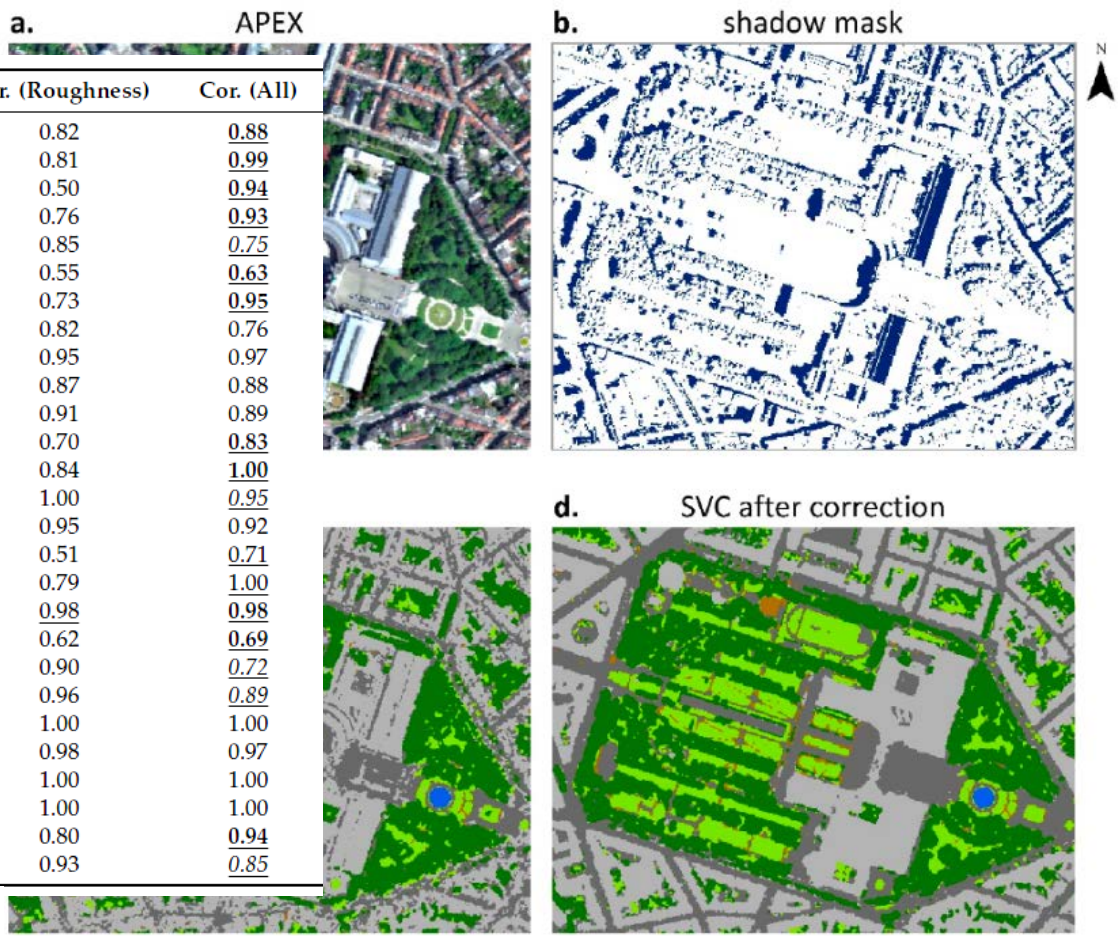

Species mapping in urban areas

Urban tree species mapping using 3.7 m AVIRIS plus LiDAR data, later on used for LAI and carbon mapping (Alonzo et al., 2014)

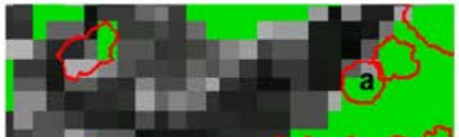

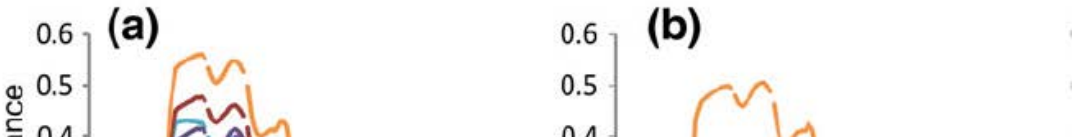

"We find that the addition of lidar data are critical for mapping species with small crowns and those with unique crown forms."

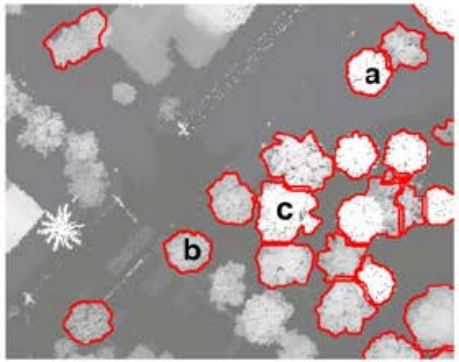

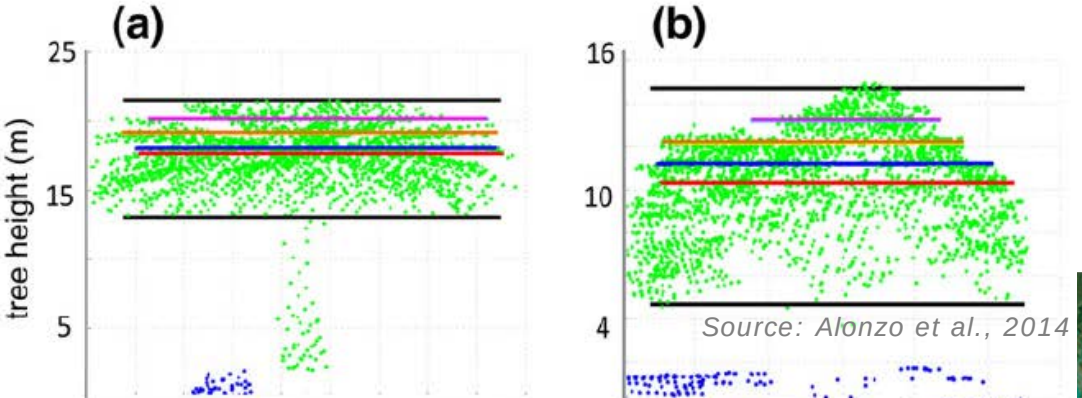

Source: Alonzo et al., 2014

Mapping class fractions from spectral data

Given the high number of mixed pixels in spaceborne data, quantitative mapping appears more useful than traditional classification to describe urban composition.

Concepts for quantitative mapping most often assume a linearly mixed spectrum, which can be decomposed into “pure” components, e.g. by linear spectral mixture analysis.

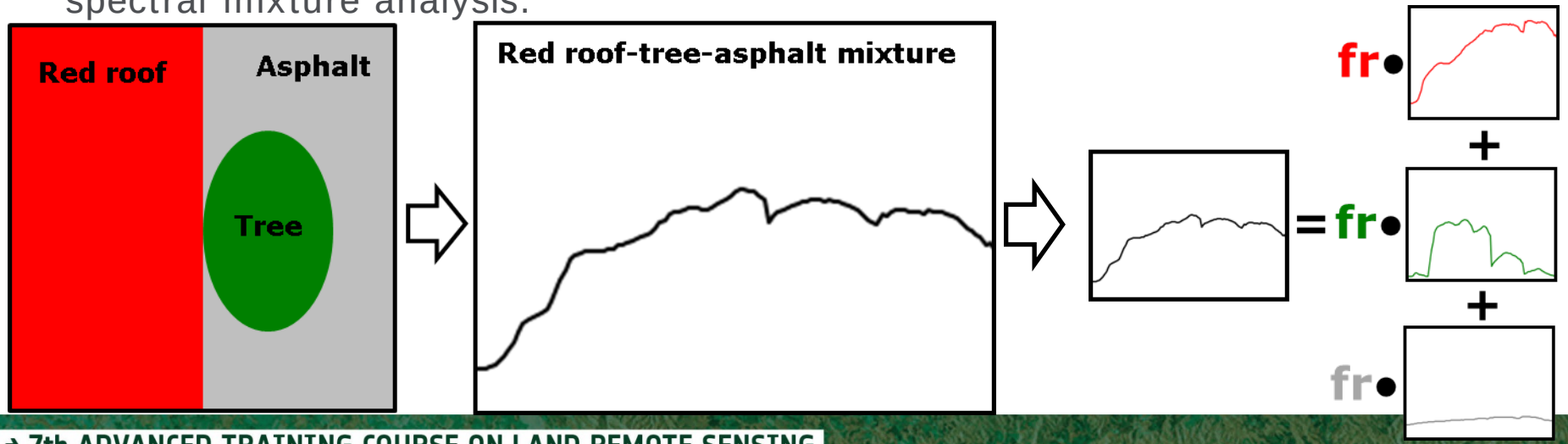

Mapping class fractions from spectral data

SVRsynthmix (*Okujeni, van der Linden et al., 2013, 2015, 2017*)

Machine learning algorithms (e.g. for classification and regression) were shown to produce robust and accurate results with spectral data and overcome statistical approaches, like spectral mixture analysis.

Regression requires fractional training data, which is usually not available.

This challenge is coped with by creating synthetic mixtures with known labels, which serve as training data for the supervised mapping approach.

Linear mixing is assumed and binary ternary mixtures of pure components are performed.

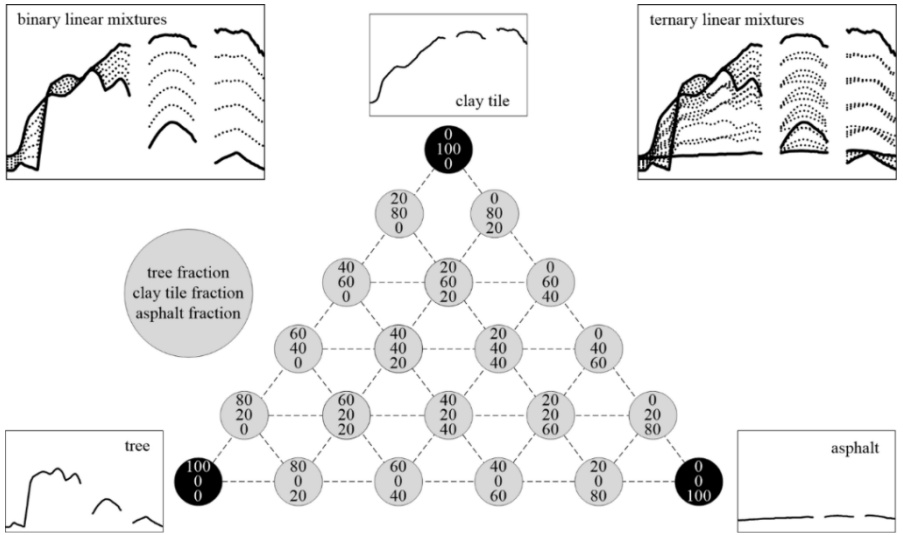

Source: Okujeni et al., 2017

Mapping class fractions from spectral data

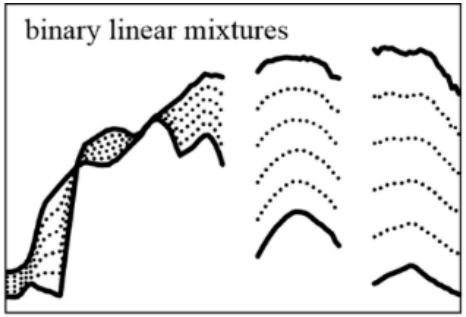

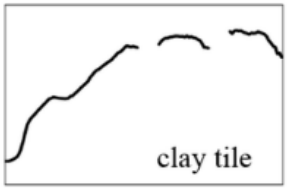

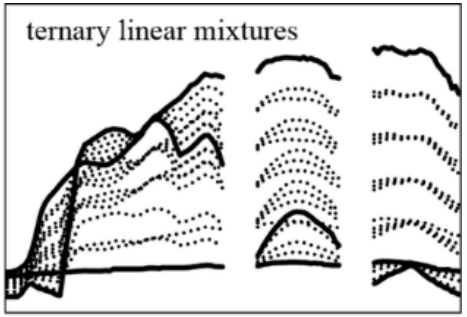

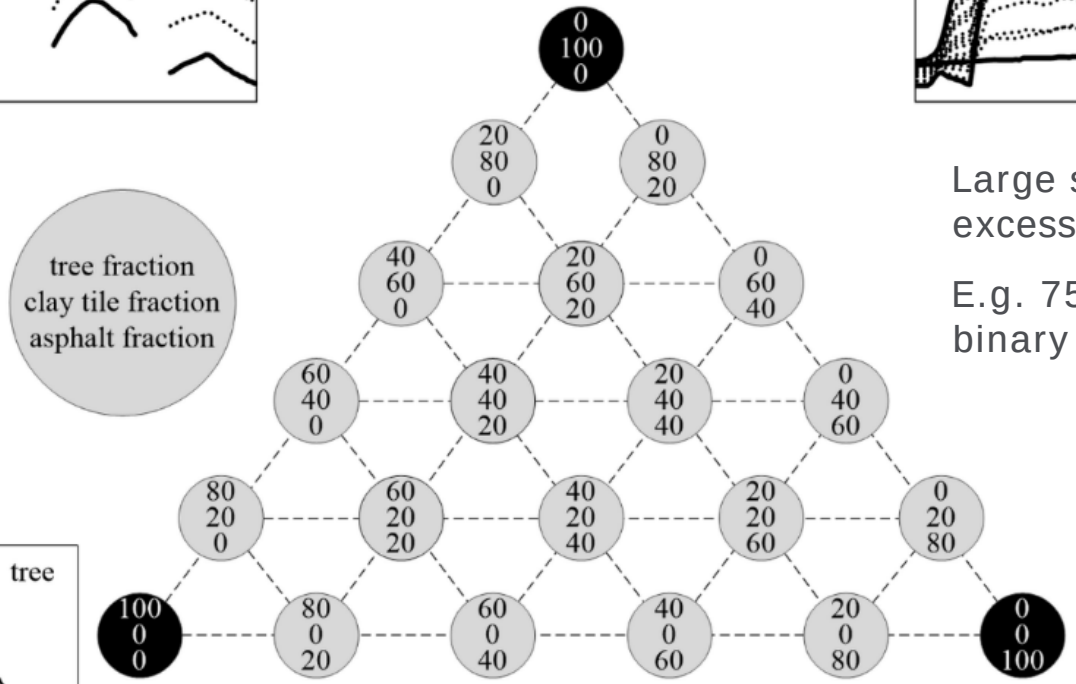

Large spectral libraries result in an excessive amount of samples.

E.g. 75 spectra result in ~400.000 binary and ternary mixed spectra

Source: Okujeni et al., 2017

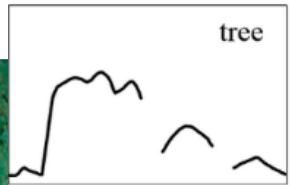

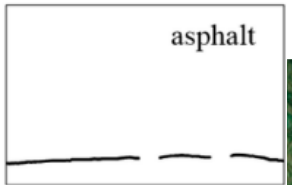

Mapping class fractions from spectral data

All VIS components can be modelled at high accuracy using SVR with synthetic mixtures.

The decrease in accuracy from 9 m to 30 m is relatively low.

EnMAP data leads to slightly better results than Landsat data.

Results for soils (not shown) are comparable.

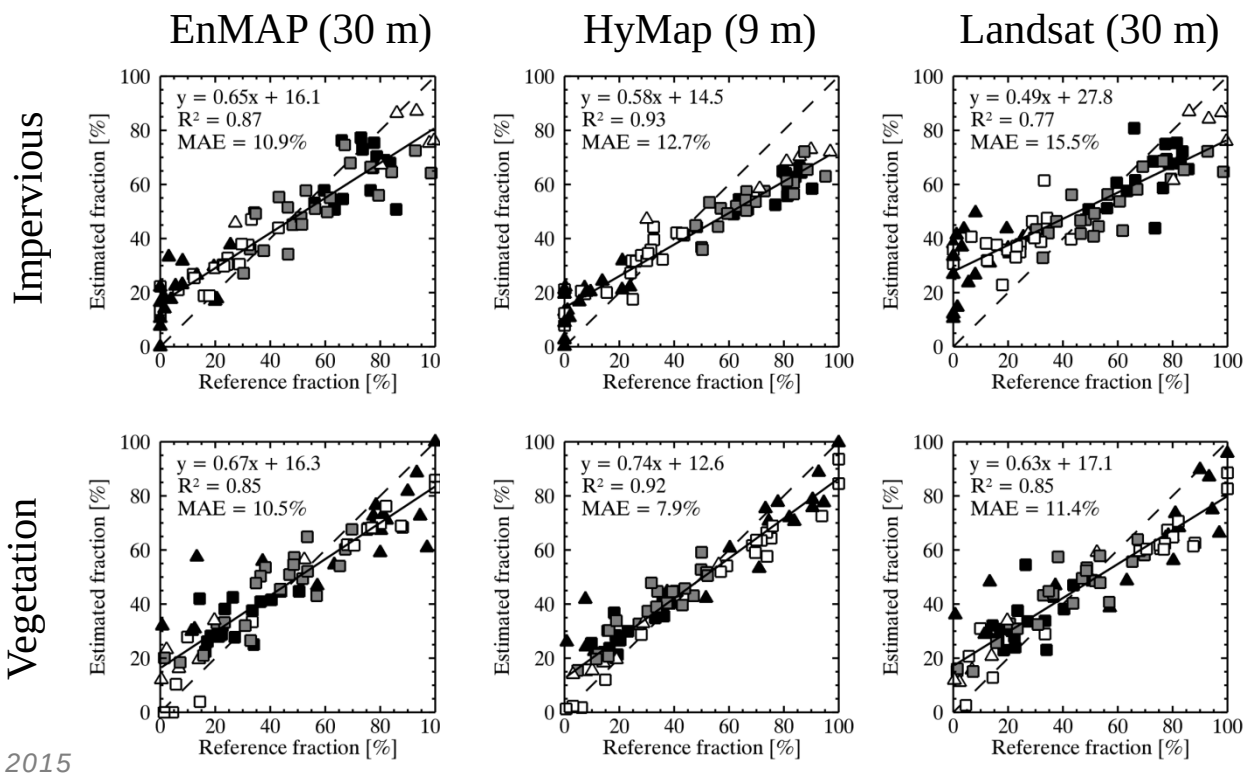

Source: Okujeni et al., 2015

Mapping class fractions from spectral data

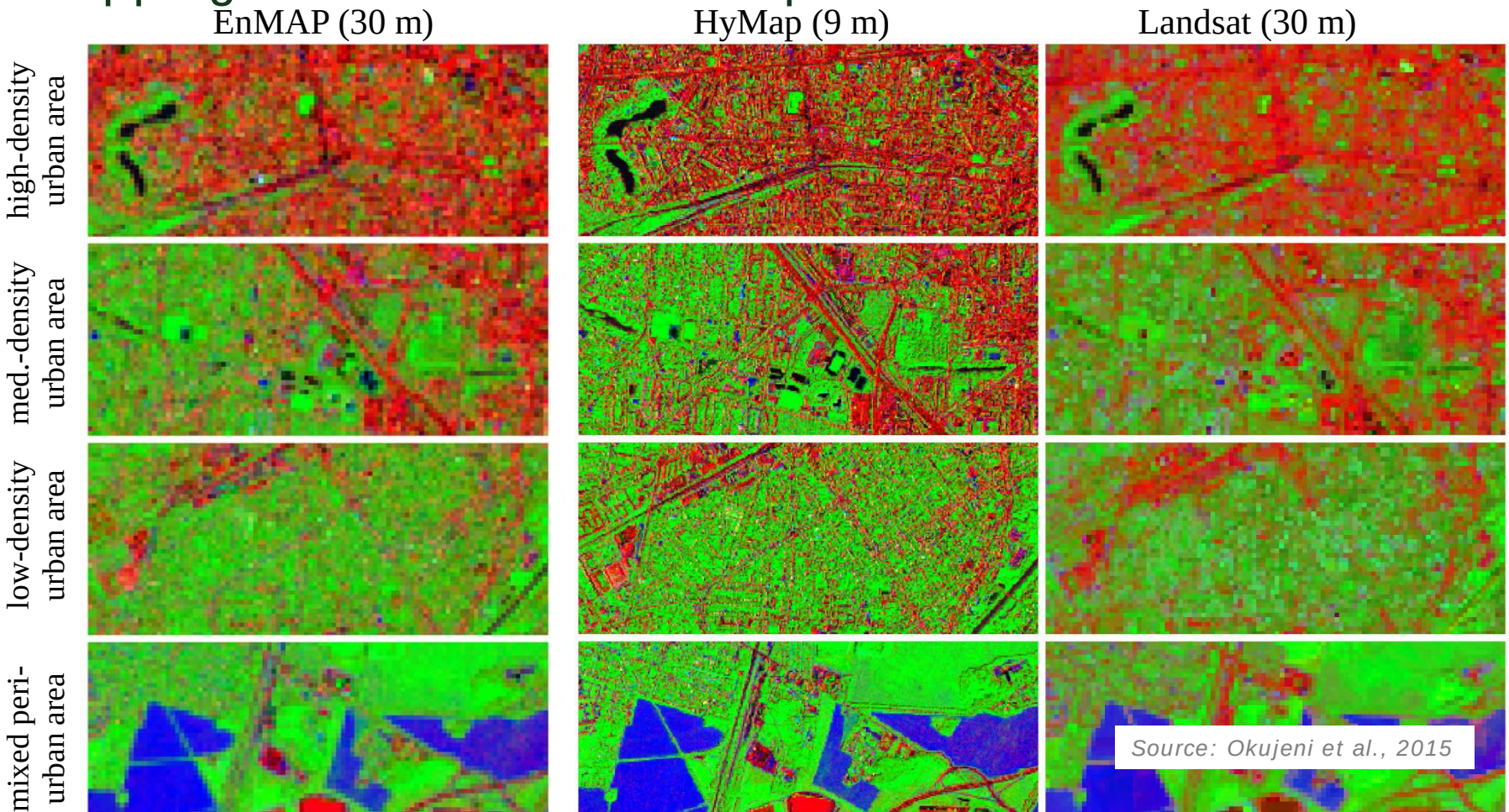

Mapping class fractions from spectral data

The SVR with synthetic mixtures allows extending the VIS framework for two vegetation and impervious types, although a clear decrease in accuracies can be observed for tree cover.

This time, the accuracy from EnMAP is clearly better than for Landsat.

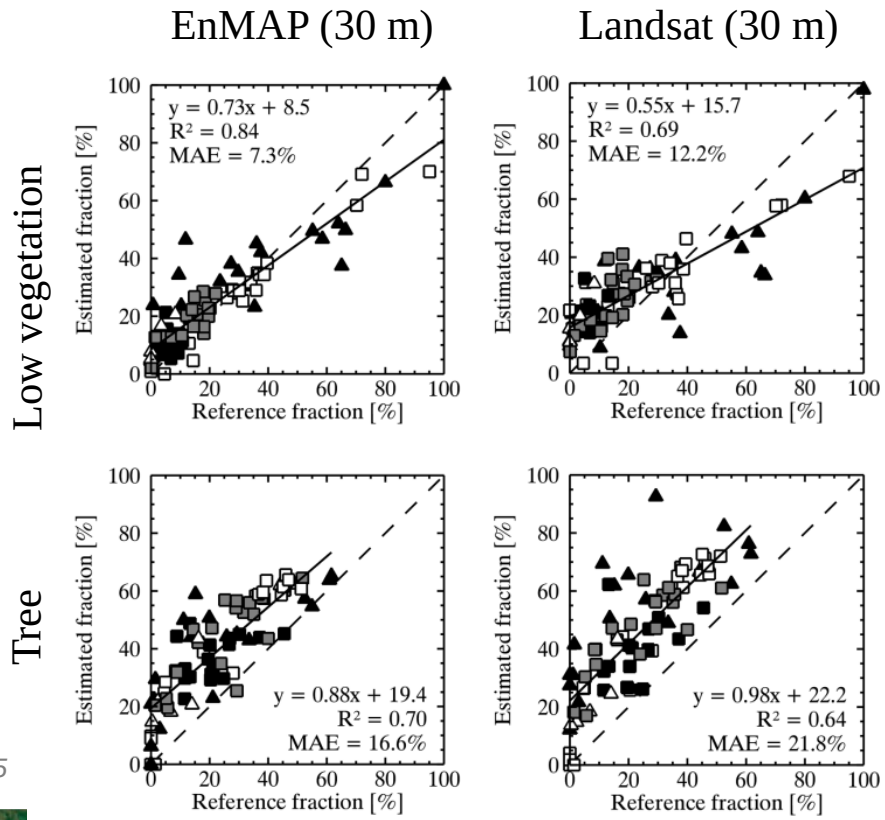

Source: Okujeni et al., 2015

Mapping class fractions from spectral data

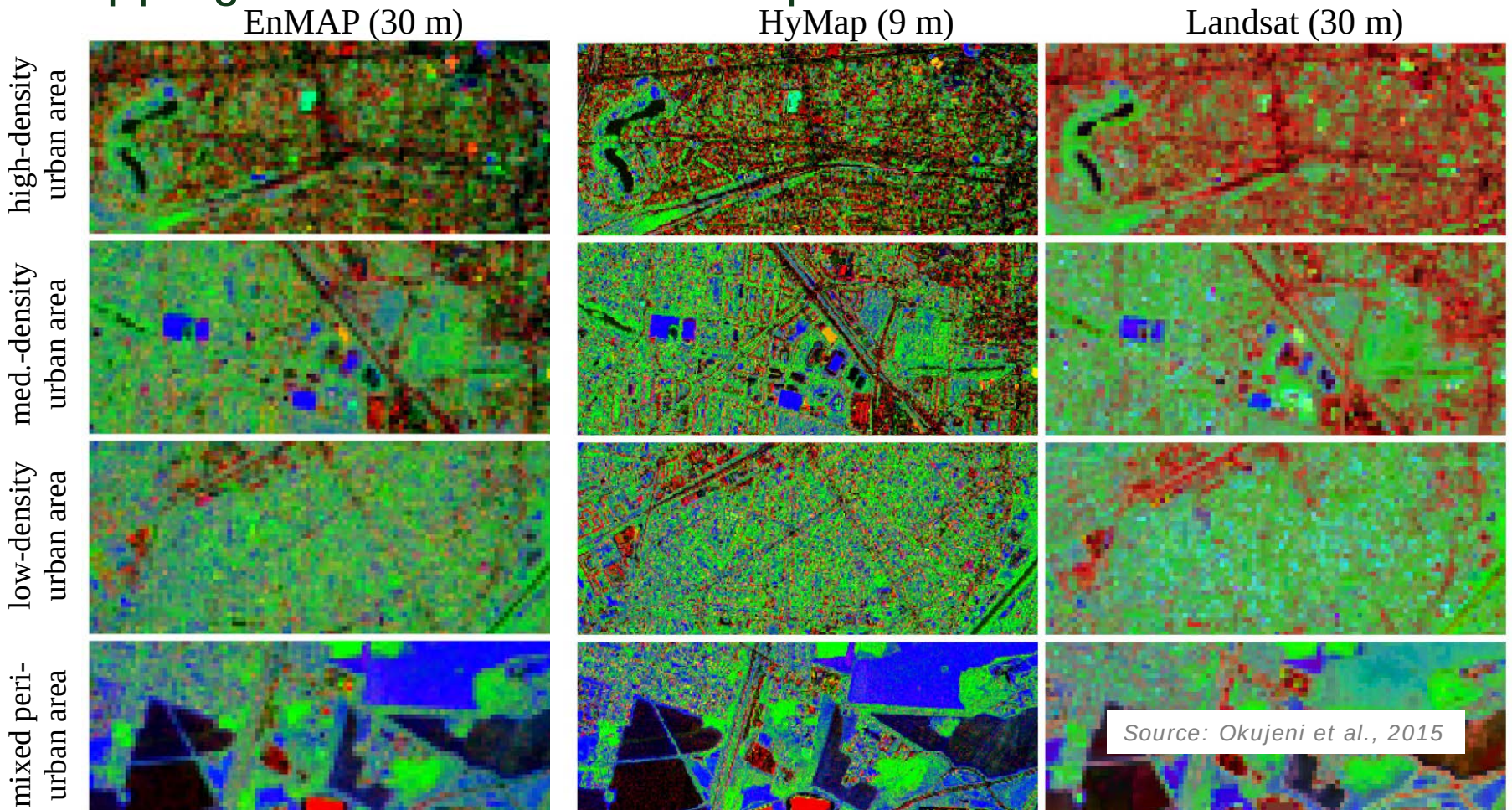

Mapping class fractions from spectral data

UEIS Impervious map

EnMAP Impervious map

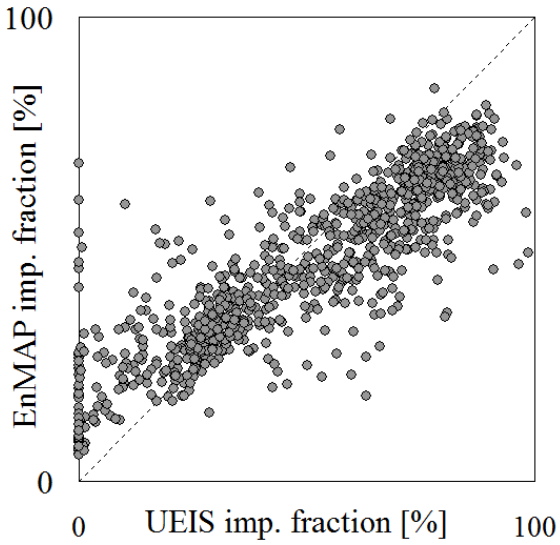

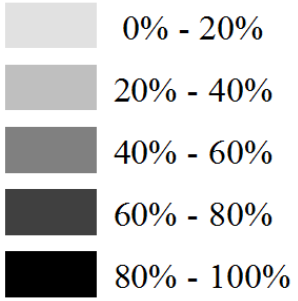

References

Small, Okujeni, van der Linden, Waske (*in press*). In S. Liang: Comprehensive Remote Sensing. Elsevier.
Alonzo *et al.* (2014). Remote Sensing of Environment, 148, 70-83.
Griffiths *et al.* (2010). Remote Sensing of Environment, 114, 426-439.
van der Linden *et al.* (2007). Journal of Applied Remote Sensing, 1.
Okujeni, van der Linden *et al.* (2013). Remote Sensing of Environment, 137, 184-197
Okujeni, van der Linden, Hostert (2015). Remote Sensing of Environment 108, 69-80.
Okujeni, van der Linden *et al.* (2017). J. of Selected Topics in Applied Remote Sensing, 10, 1640-1650.
Priem, Canters (2016). Remote Sensing, 8, 787
Ridd (1995). Int. Journal of Remote Sensing, 16, 2165-2185.
Small (2005). Int. Journal Remote Sens., 26, 661-681.
Small, Elvidge (2012). Int. Journal of Applied Earth Observation and Geoinformation. 22, 40-52.
Taubenböck *et al.* (2012). Remote Sensing of Environment, 117, 162-176.
United Nations (2014). World polulation prospects. https://esa.un.org/unpd/wpp/

If not indicated differently, figures are taken from the dissertations of S. van der Linden and A. Okujeni. See edoc.hu-berlin.de.

Thank you for your attention!

Geomatics Lab @ HU Berlin

Supported by:

Federal Ministry
for Economic Affairs
and Energy

EnMAP
Hyperspectral Imager

UrbanEARS
Belgian Science Policy Office
belspo

on the basis of a decision
by the German Bundestag

@HumboldtRemSens